



Review

Electrochemical Biosensors for Detection of MicroRNA as a Cancer Biomarker: Pros and Cons

Maliana El Aamri ^{1,†}, Ghita Yammouri ^{1,†}, Hasna Mohammadi ¹ , Aziz Amine ^{1,*} and Hafsa Korri-Youssoufi ²

¹ Laboratory of Process Engineering & Environment, Faculty of Sciences and Techniques, Hassan II, University of Casablanca, B.P.146, Mohammedia 28806, Morocco; maliana.elaamri@etu.fstm.ac.ma (M.E.A.); ghita.yammouri-etu@etu.univh2c.ma (G.Y.); hasna2001fr@yahoo.fr (H.M.)

² Université Paris-Saclay, CNRS, Institut de Chimie Moléculaire et des Matériaux d'Orsay (ICMMO), Equipe de Chimie Biorganique et Bioinorganique (ECBB), Bât 420, 2 Rue du Doyen Georges Poitou, 91400 Orsay, France; hafsa.korri-youssoufi@universite-paris-saclay.fr

* Correspondence: azizamine@yahoo.fr

† These authors contributed equally to this work.

Received: 26 October 2020; Accepted: 18 November 2020; Published: 20 November 2020



Abstract: Cancer is the second most fatal disease in the world and an early diagnosis is important for a successful treatment. Thus, it is necessary to develop fast, sensitive, simple, and inexpensive analytical tools for cancer biomarker detection. MicroRNA (miRNA) is an RNA cancer biomarker where the expression level in body fluid is strongly correlated to cancer. Various biosensors involving the detection of miRNA for cancer diagnosis were developed. The present review offers a comprehensive overview of the recent developments in electrochemical biosensor for miRNA cancer marker detection from 2015 to 2020. The review focuses on the approaches to direct miRNA detection based on the electrochemical signal. It includes a RedOx-labeled probe with different designs, RedOx DNA-intercalating agents, various kinds of RedOx catalysts used to produce a signal response, and finally a free RedOx indicator. Furthermore, the advantages and drawbacks of these approaches are highlighted.

Keywords: microRNA; electrochemical biosensor; catalysts; RedOx indicator; cancer biomarker

1. Introduction

Cancer has been the focus of intense scientific research in recent decades because it includes more than 14 million new cancer cases as well as 8.2 million deaths annually, which makes it one of the most fatal diseases in the world. It is a complex disease characterized by abnormally large cell proliferation, or malignant tumor, formed from the transformation by mutation or genetic instability of an initially normal cell [1]. Attacking some tumor cells that are the source of the disease requires early diagnosis to control and treat them.

The detection of cancer in the early stage of its evolution greatly increases the chances of the treatment success [2]. Indeed, it is based on screening, and on educating patients about early diagnosis. There are many methods of detecting cancer, but the challenge is whether these tests are used to help identify cancer and give an appropriate treatment at an early stage. Among these methods, the most effective ones include imaging exams [3,4] including, radiography, echography, computed tomography scan, magnetic resonance imaging, and positron emission tomography. However, biochemical methods based on the detection and quantification of biomarkers could give an early diagnosis. Biomarkers are defined as substances found naturally in the cells, tissues, or fluids of the human body and present in abnormal amounts in people with cancer or a precancerous condition [5]. Cancer biomarkers could

be specific to a single type of cancer or associated with more than one type of cancer [6]. Various cancer biomarkers are known and some of the associated ones with cancer diagnosis are summarized in Table 1.

Table 1. Biomarkers associated with the diagnosis and prognosis of cancer.

Cancer	Biomarkers	Reference
Breast	BRCA1, BRCA2, MUC1, CEA, CA 15-3, CA 27, CA29, EGFR, EpCAM, HER2; miRNA-21, miRNA-373, miRNA-182, miRNA-1246 and miRNA-105	[7–10]
Prostate	PSA, Sarcosine; TEMPRSS2; miRNA-21, miRNA-141, miRNA-375	[11–13]
Brain	MDM2;	[14]
Pancreas	CA 19-9, PAM4; miRNA-21, miRNA-155, miRNA-196	[15,16]
Gastric/Stomach	CA72-4, CA19-9, CEA, IL-6; PVT1; miRNA-21, miRNA-331, miRNA-421	[17,18]
Liver	AFP, DCP, GP73; miRNA-21, miRNA-122, miRNA-16	[19]
Ovarian	CA 125 (MUC-16), CEA, Claudin-4;	[20,21]
Lung	ANXA2, CEA, Chromogranin A, CA 19-9, CYFRA 21-1 (CA-19 fragment), NSE, SCC, SAA1, HER1; P53, P16, Ras genes, Telomere length and telomere-related genes, EGFR gene (c-ErbB-1 and c-ErbB-2); miRNA-21 (in sputum)	[22–26]
Neck	MGMT gene	[27]

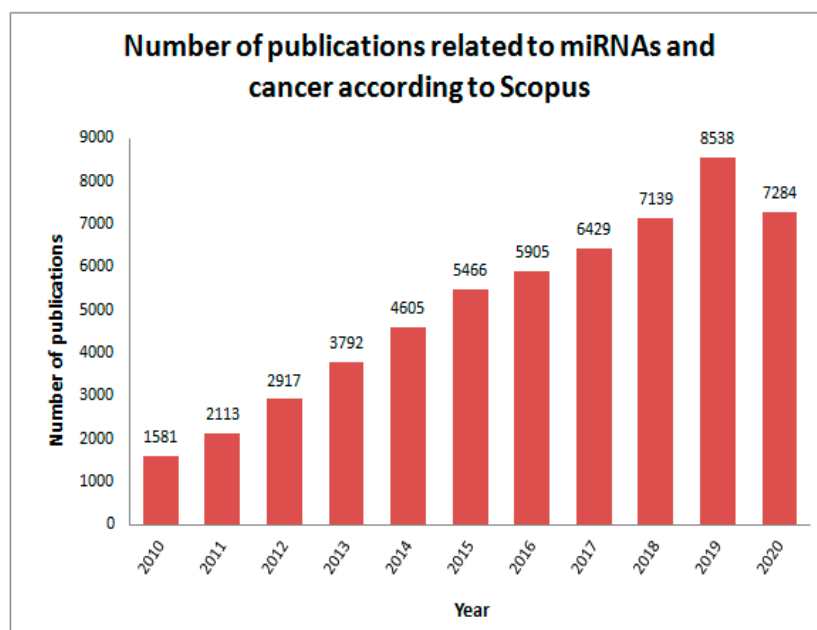
Abbreviations: BRCA1, breast cancer 1 gene; BRCA2, breast cancer 2 gene; MUC1, mucin1; CEA, carcinoembryonic antigen; CA, cancer antigen; EGFR, epidermal growth factor receptor; EpCAM, epithelial cell adhesion molecule; HER, human epidermal growth factor receptor; miR, micro-RNA; PSA, prostate-specific antigen; PAP, prostatic acidic phosphatase; MDM2, murine double minute 2; AFP, α -1-fetoprotein; DCP, des- γ -carboxyprothrombin; GP73, golgi protein 73; ANXA2, annexin A2; NSE, neuron-specific enolase; SCC, squamous cell carcinoma antigen; SAA1, serum amyloid A1; P53, protein suppressor gene; MGMT, o^6 -methylguanine DNA methyltransferase.

In recent decades, researchers have focused on microRNA (miRNA) as a cancer biomarker. According to Scopus, and over the years, miRNAs have generated a high amount of interest in the cancer research area, as described in Scheme 1. The number of papers related to miRNA detection as a cancer biomarker was about 650 in 2019, showing the high interest in miRNA analysis.

The interest in targeting miRNAs as cancer biomarkers is related to their biochemical properties and their large amount in biological fluids; they allow easy detection avoiding sample treatment complications.

MiRNAs are small non-coding single-stranded sequences constituted of 18–25 nucleotides [28]. The expression level of the miRNAs is strongly correlated with the onset and development of diseases, including cancer, diabetes, and heart disease [29,30].

The conventional methods used for the quantification and identification of miRNAs are real-time quantitative polymerase chain reaction (RT-qPCR), DNA microarray, Northern blot techniques, and deep sequencing [31]. In general, they have good sensitivity and high specificity, but the methods are complex and need a high level of technology that requires costly equipment and materials, qualified personnel for the assay, and is time consuming [32].



Scheme 1. Number of publications in the field of micro-RNAs and cancer in the period between 2010 and 2020 (www.scopus.com, analyzed by years) (consulted 25 October 2020) (Keywords: micro-RNAs, cancer).

For this reason, the development of other more efficient and less expensive emerging techniques is important and vital for cancer diagnosis and therapy. A variety of methods providing high sensitivity and specificity, and that are easy to handle have been recently developed based on various direct detection methods such as photoelectrochemical, localized surface plasmon resonance, and electrochemical biosensors [33].

Electrochemical biosensors present interest because they can be easily miniaturized, and allow mass-production at a low cost. They could be modified with various recognition elements and are greatly used as versatile devices for nucleic acids-based biosensors development (E-DNA). In addition, such biosensors have demonstrated convincing results with versatile approaches based on newly developed materials and nanomaterials, natural organic and bioorganic polymers, electroactive molecules, catalysts, and biocatalysis, etc. [34–36].

In recent years, reviews of electrochemical miRNA biosensors at various viewpoints have been published. Therefore, various strategies based on multi-functional nanomaterials in miRNA biosensors were reported [37,38]. For example, Chen et al. [31] discussed the use of nanomaterials and oligonucleotides as amplification strategies for miRNA detection. Besides, Michael et al. [39] focused more on electrochemical biosensors based on using various combinations of oligonucleotide strategies. Furthermore, Mohammadi et al. [40] reviewed the various amplification strategies based on nanomaterials, oligonucleotides, and enzymes for miRNA analysis and their different possible combinations.

In this review, we provide a compressive overview of various detection approaches of miRNA detection in the literature from 2015 to 2020 following their prevalence. The review focuses on direct miRNA electrochemical biosensing systems based on the RedOx marker. These approaches are based on the RNA biosensors with (i) an electroactive labeled DNA probe sequence, (ii) the use of a catalyst that generates RedOx specie, (iii) the system with DNA RedOx intercalating agent, (iv) the employment of free RedOx indicator and finally, other methods of detection free of the RedOx marker. Various detection approaches are discussed in terms of analytical performances, particularly sensitivity and limit of detection (LOD). We highlight the advantages and drawbacks of these detection approaches. The challenges and successes of these assays are discussed.

2. Electrochemical Biosensor Based on Electroactive Labeled Probe Sequence

Electroactive species-labeled DNA probe sequence strategies are widely used for miRNA detection. They provide direct RedOx current response related to the signal variation after the miRNA hybridization. These electroactive species can be inorganic molecules as well as organic ones. For example, metals such as gold nanoparticles [41], silver nanoparticles [42], cadmium [43], and plumb [44] were employed as an inorganic RedOx probe. Organic molecules including, thionine (Thi) [45], ferrocene (Fc) [46], and methylene blue (MB) [47] were mostly used. Indeed, the RedOx molecule could be labeled to the probe sequence directly or with the help of a linker. These methods of labeling will be detailed in this section.

2.1. Direct Labeling

Biosensors with direct current response readout are based on short strand DNA probes complementary to the target sequence (miRNA) labeled with molecules of RedOx activity. These labeled probes are firstly immobilized at the surface of the electrode through surface chemistry. The recognition of the miRNA target sequence generates a variation in signal response of the RedOx molecule, which is proportional to miRNA concentration. The literature data show that the labeled DNA probes could be presented with different types of architecture (Figure 1) providing a decrease (ON-OFF signal) or increase (OFF-ON signal) in current response after the hybridization step, starting with a basic design (Figure 1A) and progressing to other more advanced designs based on the elimination of the labeled probe sequence (Figure 1B), the use of a secondary probe labeled with RedOx molecule (Figure 1C) and finally, the use of a two-probe labeled sequence (Figure 1D).

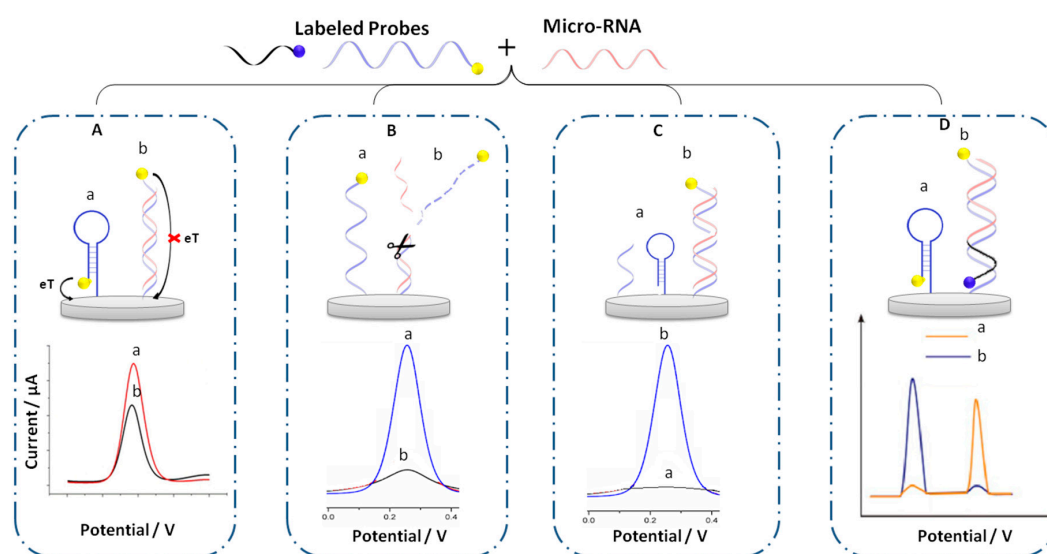


Figure 1. Different architecture of electrochemical biosensors based on labeled probe with RedOx molecules before and after hybridization. (A) Basic design; (B) elimination of labeled probe sequence; (C) the use of secondary probe labeled with RedOx molecule; (D) the use of two-probe labeled sequence, (a) before and (b) after hybridization.

2.1.1. Basic Design

This method is based on the use of a labeled capture DNA probe, which is immobilized at the electrode surface and labeled with a RedOx molecule at the other extremity. However, as shown in Figure 1A, the presence of target miRNA after a hybridization reaction leads to a variation of the distance from the RedOx molecule to the electrode surface, which hampers electron transfer and leads to a decrease in current response (ON-OFF systems). Following this approach, Jou et al. [48], immobilized hairpin DNA probes on a screen-printed carbon electrode (SPCE) modified with AuNPs. The hairpin was labeled at the 5' end position with MB as a RedOx signal reporter. Before hybridization,

the MB is near the electrode surface and thus the electron transfer between the MB and the electrode is possible, so the oxidation response of MB is very high. However, in the presence of the miRNA target, and after displacement amplification reaction and duplex-specific nuclease (DSN), the hairpin was opened indicating the presence of the target, which generates a distance between the RedOx molecule and the surface resulting in a decrease in MB oxidation signal. This method showed an LOD of 3.57 fM for miRNA-155 as a blood cancer biomarker. To improve the sensitivity of detection, Miao et al. [49] used a DNA hairpin immobilized directly on a gold surface electrode and marked with MB at the 5' end. They introduced the tris (2-carboxyethyl) phosphine hydrochloride reducer (TCEP) providing an enhanced electrochemical signal of MB. The oxidation signal enhancement is based on the activation of MB by reducing its oxidized form in the presence of TCEP. This method allows an improvement of the LOD where 3.2 aM is demonstrated. Yammouri et al. [47] demonstrated a biosensor for miRNA cancer markers with LOD of 1 fM using a basic design where MB-labeled DNA probe sequences and well adapted surface chemistry based on pencil carbon were used. This allows a signal of readout after DNA hybridization without using TCEP as a mediator. The aforementioned methods based on ON-OFF systems lead to an increase in the error of the measurement at low miRNA concentrations. To overcome this problem, a specific architecture of DNA such as loop DNA or DNA stream could be used and the hybridization, in this case, brings the RedOx marker closer to the surface leading to an increase in current response (OFF-ON systems). Wang et al. [50] relied on the "OFF-ON" systems offering a femtomolar detection limit of miRNA-122. In this case, a triple-stem DNA-labeled MB was used. This structure locks MB away from the electrode, and thus blocks electron transfer pathways. Indeed, the signal is turned on only upon the recognition with the target miRNA, which leads to a significant signal response of MB after the hybridization reaction.

2.1.2. Response Based on the Elimination of the Labeled Probe

In this strategy, the labeled probes are released after their hybridization with miRNA targets as shown in Figure 1B. Various methods were employed to achieve this approach. The more popular method is the use of a cleaving agent such as endonucleases [51], duplex-specific nuclease [52], or calcium ions [53] to remove the hybridized duplexes and eliminate the labeled probe from the electrode surface.

The removal could also be obtained by desorption of dsDNA bearing the labeled probe after the hybridization reaction of miRNA due to lower affinity of dsDNA–RNA to the surface (Figure 2). In this case, biosensors based on carbon nanomaterials were demonstrated such as graphene oxide [42] or SWCNTs [46] where the adsorbed ssDNA probe has more affinity to the nanomaterial than dsDNA–RNA does.

Another method uses the competition of miRNA target with two DNA probes in which one is non-labeled and could be hybridized with an MB-labeled duplex reporter. When miRNA target is present, its hybridization reaction with a non-labeled attached probe takes place leading to the displacement of the labeled reporter from the surface [54].

A 2D DNA nanoprobe (DNP) and enzyme-free-target-recycling amplification method based on toehold-mediated strand displacement reactions (TSDRs) was also used to achieve the release of Fc-labeled DNA strands in the case of miRNA-21 detection. The method is based on the displacement of the Fc-labeled DNA strands from the glassy carbon electrode (GCE)/gold nanoparticles (AuNPs) surface after TSDRs, resulting in a decrease in the electrochemical signal. The proposed biosensor has an LOD of 0.31 fM and can be regenerated four times [55].

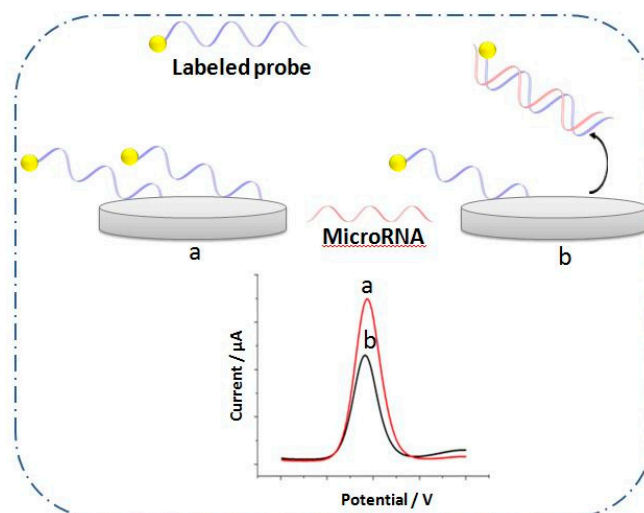


Figure 2. Architecture of electrochemical biosensor based on destroying the adsorption of the labeled probe after hybridization step on the electrode surface (a) before and (b) after hybridization.

The previous methods described are simple in the design of the biosensors but lead to a decrease in current signal upon miRNA hybridization with “On-OFF systems”. The detection with increasing response signals based on “OFF-ON Signal” was also demonstrated in the case of the release of the labeled DNA probe. Thus, Fu et al. [56] developed a biosensor based on a homogenous system of detection without immobilization of the ssDNA probe, permitting the reduction in the preparation time of the biosensor. Indeed, the biosensor is based on the negatively charged probes marked with MB at the 3’ end and a negatively charged indium tin oxide (ITO) electrode surface where DNA cannot diffuse easily to the surface due to electrostatic repulsion and the low electrochemical signal of MB is detected. After hybridization, the duplex DNA probe-miRNA was cleaved by DSN hybridization and miRNA continues the second cycle of hybridization cleavage; in the end, this released many short fragments of MB-labeled oligonucleotides with less negative charges, which easily allowed the diffusion on the electrode surface, resulting in a high electrochemical signal.

2.1.3. The Use of Secondary Probe Labeled with RedOx Molecule

This strategy is based on the use of two DNA sequences, the first one is a DNA probe immobilized on the electrode surface, which is targeting a part of miRNA, and the second one is a DNA probe labeled with RedOx molecule targeting the other part of miRNA. After hybridization, the secondary probe labeled with the RedOx molecule leads to a positive signal readout. The principal of this strategy is presented in Figure 1C. This approach was demonstrated by Miao et al. [57] with a biosensor in which an miRNA opened a hairpin capture probe that was immobilized on a gold electrode, while a second probe labeled with silver nanoparticles (AgNPs) was hybridized with the capture probe. A Klenow fragment initiates polymerization of the labeled probe and leads to a release of miRNA. The obtained biosensor provides intense electrochemical signals reaching an LOD of 0.4 fM. Other groups used the same method and amplified the signal readout by the use of rolling circle amplification (RCA) and several probes labeled AgNPs. This leads to an increase in the number of AgNPs on the electrode surface reducing the LOD to 50 aM [58]. Otherwise, with the same principle of detection, other nanoparticles could be used such as CdTe quantum dots (CdTe QDs) instead of AgNPs. With CdTe, a biosensor of miRNA with a very low LOD of 33 aM was demonstrated [59].

An interesting approach was demonstrated for the simultaneous detection of miRNAs using the tetrahedron DNA (TDN) nanostructure (Figure 3A) [60]. This biosensor involved an advanced DNA structure such as TDN which is immobilized on the surface and hybridized with DNA circle as a capture probe presenting many target recognition domains. In the presence of two target miRNAs, and with the assistance of two DNA probes, the mimetic proximity ligation assay (mPLA) can be

triggered. The last step is the capturing of two labeled DNA probes labeled with Fc and MB which generate two electrical signal responses. The LOD obtained is in an attomolar range for miRNA-21 and miRNA-155 of 18.9 aM and 39.6 aM, respectively.

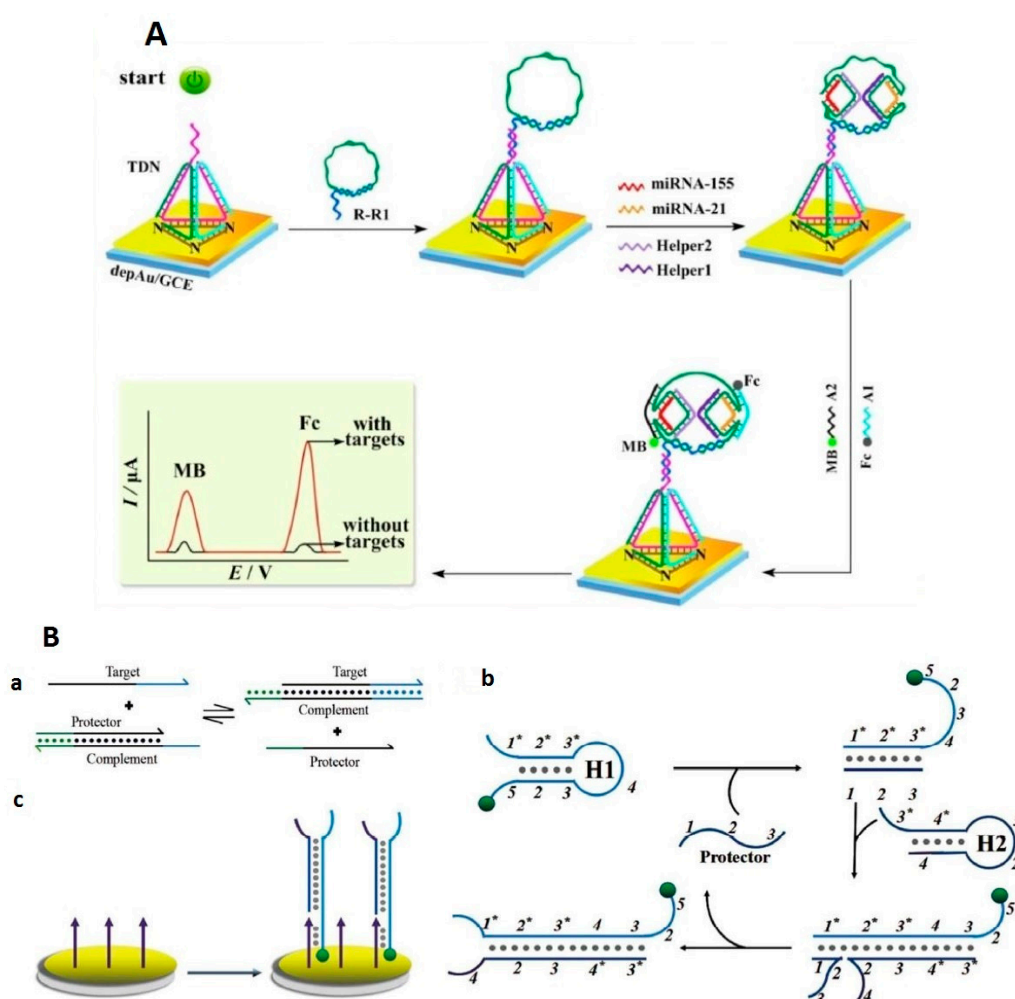


Figure 3. Example of the biosensor with an electrochemical response based on “signal ON”, (A) detection approach using DNA circle for simultaneous detection of miRNA (reproduced with permission from the publisher [60]); (B) scheme of the biosensor design using (a) strand displacement reaction to generate protector output (b) catalytic hairpin assembly to generate H₁/H₂ duplex output and (c) electrochemical signal generation procedure (reproduced with permission of Royal Society of Chemistry) [61].

Another design of an miRNA biosensor was demonstrated by exploiting the small size of the RedOx molecule, which allows them to be closer to the electrode surface, resulting in an intense RedOx signal. This was obtained by sophisticated design strategies based on coupling the strand displacement reaction and catalytic hairpin assembly recycling (see Figure 3B) [61] or by using an isothermal target recycling amplification strategy [62].

2.1.4. Response Based on Two Labeled Probes

This strategy is based on two probes labeled with different RedOx molecules, in which one is placed near the surface electrode and the second is far from the surface. The signal obtained after RNA hybridization leads to a response where one of the RedOx molecules increases because it becomes closer to the surface and the second one decreases according to the concentration of the hybridized DNA. The final response is a ratio between the two responses (Figure 1D). Various biosensors for miRNA detection were developed following this method in addition to the amplification strategy [63]

(see Figure 4A). Most of the developed biosensors used ratiometric electrochemical sensors to obtain a reliable experimental result, which is less sensitive to electrode surface conditions, the probe packing density, the environment, and artificial factors [64–67].

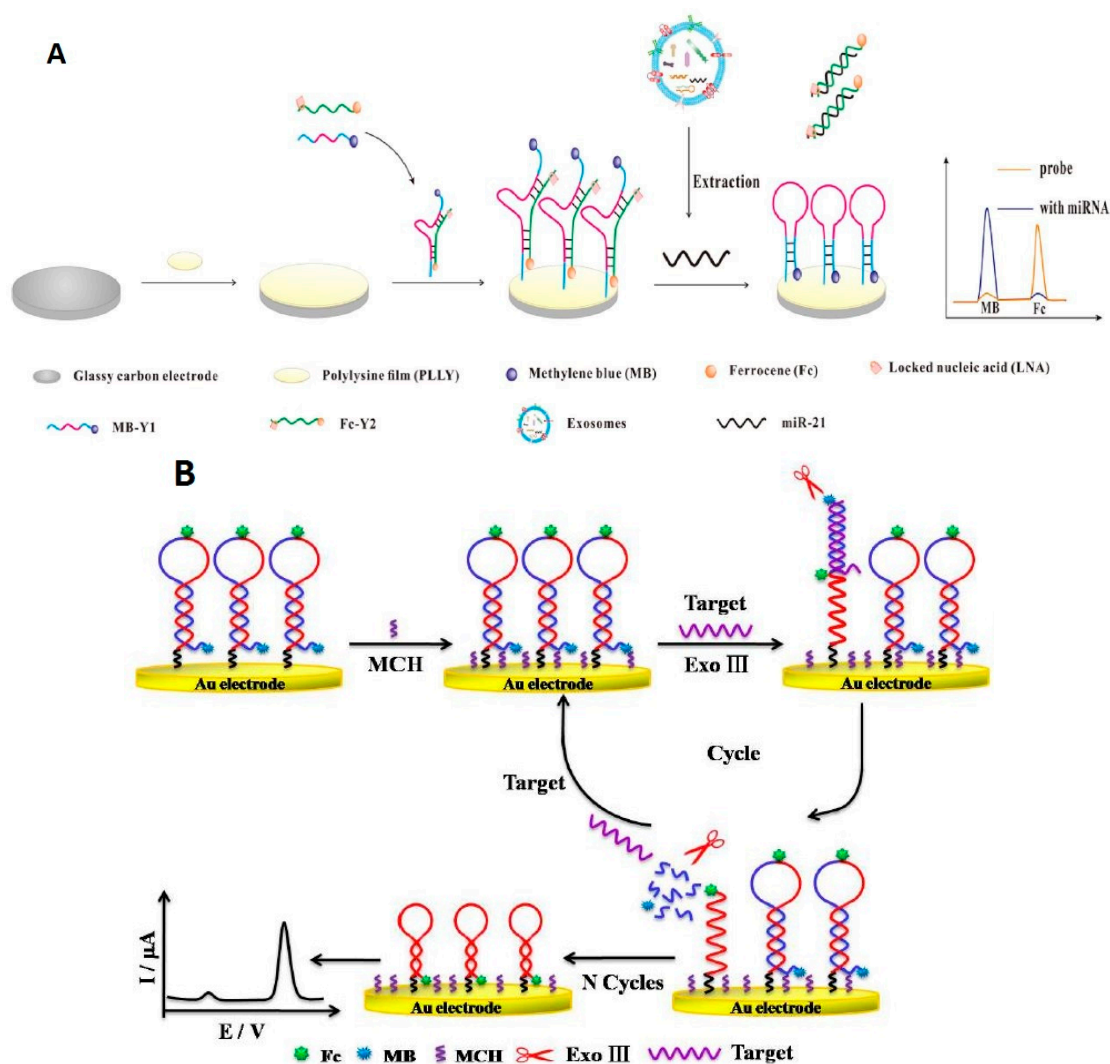


Figure 4. Example of biosensor obtained with two DNA label with two RedOx markers; (A) standard design reproduced from [68] with permission of publisher, (B) same approach using amplification strategy reproduced with permission of the publisher from [63].

Amplification strategy using exonuclease-assisted target recycling [63] (Figure 4B) or mismatched catalytic hairpin assembly (CHA) [65] can improve the signal-to-background ratio of the sensor. Using this type of ratiometric design, Zhang et al. [64] developed a more original biosensor based on bipedal DNA walkers for the detection of exosomal miRNA-21. Fc and MB RedOx probes produce a final ratiometric signal, allowing them to obtain an LOD up to 67 aM of miRNA-21. The biosensor developed was applied in a real sample and compared with other methods as RT-qPCR and was regenerated five times without signal decrease.

2.2. RedOx Molecules Linker to Nanocarriers

This strategy is based on the use of a RedOx molecule labeled to the probe through a linker such, nanomaterial, polymer, and streptavidin and leads to RedOx signal amplification leading to signal ON. This allows the immobilization of a large number of RedOx molecules after a hybridization reaction leading to the high sensitivity of the biosensor (Figure 5).

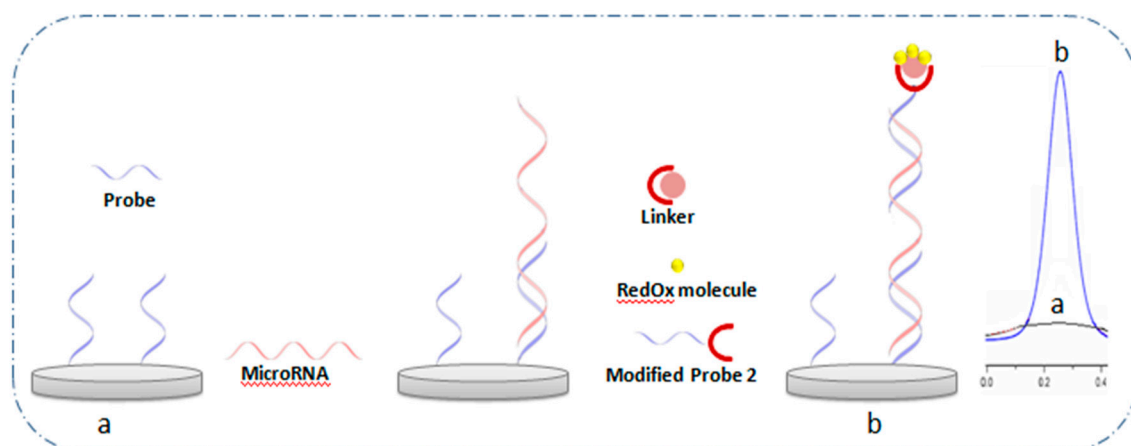


Figure 5. Architecture of electrochemical biosensor based on a RedOx molecule labeled probe via a linker molecule (a) before and (b) after hybridization.

Nanomaterials can be used as carriers of the RedOx molecule [44]. AuNPs are usually used in this case as they allow easy attachment through the thiol link. For example, AuNPs have demonstrated an amplification transducer signal conjugated to RedOx molecules such as doxorubicin [69] or cadmium sulfide nanoparticles [66], through sulfur interaction. Another example of a biosensor for miRNA-141 was demonstrated by Yuan et al. [70] where AuNPs were conjugated to Thi- and Fc-labeled hairpin capture probes immobilized on the electrode surface. In the presence of miRNA-141, an increase in the Thi signal is observed, causing a decrease in the Fc signal. The AuNPs-conjugated RedOx molecule could be linked to the capture probe sequence via streptavidin (SA). In this regard, Fc-AuNPs-SA can be used as a labeling nanocarrier for a sandwich biosensor structure. In this system, the capture DNA probes are immobilized on GCE modified with graphene oxide-AuNPs through thiol chemistry. After miRNA hybridization, a second biotinylated capture probe is hybridized. The probe bearing a nanohybrid was added for the quantization of hybridized miRNA-21. This biosensor gives a femtomolar LOD and presents good stability (63 days) [71].

Magnetic nanoparticles such as Fe_3O_4 were also employed as a reporter for RNA detection. As an example, a biosensor was developed with the objective of simultaneous detection of miRNA-141 and miRNA-21. In this case, two RedOx molecules, Thi and Fc are attached to the magnetic nanoparticle and the captured probe leading to a large number of RedOx molecules attached. In the presence of miRNAs, the hybridization chain reaction was performed, and then the DNA1/ Fe_3O_4 NPs/Thi and DNA2/ Fe_3O_4 NPs/Fc were captured by the formed dsDNA, which generate a large number of magnetic nanoprobes attached to the surface. A magnified response of currents is obtained with good stability for 4 weeks and was applied for the diagnosis of miRNA in human breast cancer cells [72].

Protein such as streptavidin could be also used as carriers of RedOx molecules. Indeed, AuNPs as RedOx molecules were conjugated to a probe sequence through streptavidin for miRNA-106a detection in the case of gastric cancer diagnosis, causing a lower LOD [41].

Most electrochemical biosensors based on electroactive species-labeled probe sequences for miRNA detection of cancer markers published from 2015 to 2020 are reviewed in Table 2 and their various analytical performances are highlighted.

Table 2. Current sensitive electrochemical biosensors using electroactive species-labeled probe sequence miRNA detection.

miRNA	labeled RedOx Molecule	Platform	Signal Amplification	Tech	Linear Range	LOD	Real-Samples Application	Ref
miRNA-141	MB	AuE	SDR	SWV	0.1fM–0.2 pM	23 aM	Human bladder cancer T24 cells	[53]
-	MB	GCE/PDDA/AuNPs	DSN	SWV	100 aM–1 nM	30 aM	human serum samples	[51]
miRNA-21	MB	GCE/CNNS/AuNPs	DSN	SWV	10 fM–1 nM	2.9 fM	Spiked human serum	[52]
MiRNA-21	MB	PtE/AuNFs	MB/barcode AuNPs	DPV	500 aM–50 pM	135 aM	spiked human serum	[73]
miRNA 21	Fc	AuE	SWCNTs	DPV	100 pM–3.5 fM	0.01 fM	Human serum	[46]
miRNA-155	Fc	GCE/Mo ₂ C/AuNPs	CHA	DPV	0.1 fM–1.0 nM	0.033 fM	Spiked human serum	[74]
miRNA-21	Fc	GCE/Mo ₂ C/NCS	SDR	Amperometric	1.0 fM–1.0 nM	0.34 fM	Spiked human serum	[75]
miRNA-21	AgNPs	GCE/GO	-	LSV	100 fM–1 nM	60 fM	serum samples from breast cancer patients	[42]
miRNA-155	AgNPs	AuE	SDR and nicking endonuclease	LSV	1 fM–1 pM	70 aM	HeLa cells, A549, human renal cubularepithelial	[76]
Hsa-miR-17-5p	AgNPs	AuE	AuNPs HCR	LSV	100 aM–0.1 nM	2 aM	HUVEC, HK-2, HeLa, MCF-7 cells	[77]
-	AgNCs	AuE	pDNA-AgDNCs@DNA/AgNCs	DPV	1 fM–1 nM	0.38 fM	spiked human serum	[78]
miRNA-21	AgNPs	AuE	SDR	SWV	200 pM–1 fM	0.4 fM	Blood sample	[79]
miRNA-155	PEIAgNPs	AuE	-	CV	200 zM–2 pM	20 zM	cancerous humann serum	[80]

Table 2. Cont.

miRNA	labeled RedOx Molecule	Platform	Signal Amplification	Tech	Linear Range	LOD	Real-Samples Application	Ref
miRNA-21	Thi	GCE/AuNPs	MWCNTs	DPV	0.1–12000 pM	0.032 pM	spiked human serum	[81]
miRNA-155	Thi	3D N-doped rGO/AuNPs	AuAgNR	DPV	10 pM–100 μM	1pM	Spiked serum samples	[45]
miRNA-21	TB	GCE/DpAu	-	SWV	1 fM–2 nM	0.3 fM	MCF-7, human breast cancer cell line	[82]
miRNA-21	Pd NPs	GCE/GO	Pd/NPs-DNALNR and CHA	DPV	1 fM–50 pM	63.1 aM	Spiked human serum	[83]
miRNA-21	Cd	GCE/Au-RGO	TPSs Ru(NH ₃) ₆ ³⁺	SWV	1.0 aM–10.0 pM	0.76 aM	spiked human serum	[69]
miRNA	CdTe/QDs	AuE	CESA 3-QD@DNA NC	DPV	5 aM–5 fM	1.2 aM	Spiked human serum	[43]
miRNA-21	MB and Fc	AuE	-	SWV	5 fM–0.1 nM	1.1 fM	MCF-7 and HeLa	[65]
miRNA-16	MB and Fc	AuE	-	SWV	0.1 pM–100 nM	16 fM	MCF-7 cells	[84]
miRNA-21	MB and Fc	GCE/PLLy	LNA/structure“Y”shape	DPV	10–70 fM	2.3 fM	MCF-7 cells	[68]
let-7a	MB and Fc	NS-grafted ITO	-	DPV	80 aM–300 fM	25 aM	Spiked human serum	[85]
miRNA-21	MB and Fc	AuE	-	DPV	0.1–100.0 fM	67 aM	breast cancer cell line MCF-7	[64]
miRNA 21	Fc	AuE/AuNPs	-	DPV	100 pM to 1fM	0.36fM	serum	[86]
-	CdSNPs	GCE	AuNPS and DSN	ASV	1 f M–100 pM	0.48 fM	HeLa	[67]
miRNA-21 and miRNA-155	MB and Fc	SPCE	Fe ₃ O ₄ @Au@HHCR	SWV	5 fM–2 nM	1.5 fM 1.8 fM	Spiked human serum	[87]

Table 2. Cont.

miRNA	labeled RedOx Molecule	Platform	Signal Amplification	Tech	Linear Range	LOD	Real-Samples Application	Ref
miRNA-21 and miRNA-155	MB and Fc	AuE	-	SWV	10 fM–5 nM 50 fM–5 nM	2.49 fM 11.63 fM	HeLa, MCF-7 and MDA-MB-231 cells	[88]
miRNA-21 and miRNA-141	Au ion and Ag ion	GCE/Neutravidin	-	SSWV	0.5–1000 pM 50–1000 pM	0.3 pM 10 pM	Spiked Serum Sample	[89]
miRNA-21 and miRNA-141	MB and Fc	SPGE/MXene/AuNPs	-	DPV	500 aM–50 nM	204 aM 138 aM	human plasma cancer patients	[90]
miRNA-1246 and miRNA-4521	Pb (II) and Cd (II)	GCE/AuNPs	PbS@ZIF-8 CdS@ZIF-8	DPV	1 fM–1 mM	0.19 fM 0.28 fM	spiked human blood	[44]

Abbreviations: Au-disk microE, gold-disk microelectrode; MB, methylene blue; TCEP, tris(2-carboxyethyl) phosphine hydrochloride; SWV, square wave voltammetry; AuNPs, gold nanoparticles; DPV, differential pulse voltammetry; AuE, gold electrode; AgNPs, silver nanoparticles; LSV, linear sweep voltammetry; CdTe QDs, CdTe quantum dots; CESA, cyclic enzymatic signal amplification; 3-QD@DNA NC, triple-CdTe quantum dot-labeled DNA nanocomposites; GCE, glassy carbone electrode; HCR, hybridization chain reaction; Mo₂CNSs, molybdenum carbide nanosheets; Fc, ferrocene; Thio, thionine; CHA, catalytic hairpin assembly; GNF@Pt, gold nanoflower/platinum electrode; SDR, strand displacement reaction; DepAu; HeLa, human cervical cancer cell line; MCF-7, human breast adenocarcinoma cell line; SPCE, screen-printed carbone electrode; Strep, streptavidine; HUVEC, human umbilical vein endothelial cells; HK-2, human renal cubular epithelial cell; A549, human pulmonary carcinoma cell line; LNA, locked nucleic acid; NCS, N-carboxymethyl chitosan; PLLy, polylysine; NS, 1-naphthalenesulfonate; ZIF-8, Zeolitic imidazolate framework, Pb, Plomb sulfide, CdS, Cadmium sulfide; CdS NPs, cadmium sulfide nanoparticles; DSN, duplex-specific nuclease; ASV, anodic stripping voltammetry; AuAgNR, gold and silver nanorod; rGO, reduced graphene oxide; Pd NPs, palladium nanoparticles; SSWV, stripping square-wave voltammetry; SPGE, screen-printed gold electrode; PDDA, polydiallyldimethylammonium chloride; CNNS, carbon nitride nanosheet; SWCNTs, single-walled carbon nanotubes; MDA-MB-231: human breast cancer cells; MWCNTs, multi-walled carbon nanotubes; AgNCs, silver nanoclosters; RGO, polyethylenimine-grafted graphene; Ru(NH₃)₆³⁺, hexamine ruthenium(III); PtE, platinum electrode; TB, toluidine blue; AuNFs, gold nanoflowers; TPSS, titanium phosphate spheres; PEI-AgNPs, polyethylenimine-silver nanoparticles, HHCR, hyperbranched hybridization chain reaction.

Direct probe labeling is an approach in which the capture probe is ready to use, therefore it facilitates biosensor's construction and reduces the required time. The linker molecule labeled probe approach permits amplification of the signal, but needs an additional step, resulting in an increase in the time and the cost of analysis.

In general, the electrochemical biosensor based on an electroactive species-labeled probe sequence is a commonly used method by researchers, due to the high stability and sensitivity. Indeed, these biosensors enable an LOD in femtomolar to attomolar range and are able to detect miRNA in a complex sample. However, most of the work on biosensors support include an additional amplification procedure or use a sophisticated electrode interface to reach high sensitivity. Additionally, this method is considered as a versatile one, permitting the development of various kinds of biosensor design with new properties. For example, it allows ratiometric dual-current signal responses that provide self-calibration. Consequently, this method can reduce the experimentally and environmental dependent factors/interferences and is effective for miRNA detection in a complex matrix. Moreover, the small size of some RedOx molecules and rational design allow them to be near the electrode surface, which could amplify the signal and detect a small amount of the biomarker. The simultaneous detection was also demonstrated with a simple approach where various biomarkers could be detected at the same time. The direct oxidation/reduction of these molecules without the need of adding other reagents or specific temperature conditions allows them to act as a point of care test. Despite, the above-mentioned advantages, there are a risk of contamination with these molecules and the use of toxic molecules such as cadmium as labeling probe sequence should be avoided for environmental pollution. Concerning the stability of the biosensor with such a design, few works describe these aspects and the stability time is demonstrated between 7 and 30 days depending on the design. Thus, more studies should be highlighted to demonstrate the long-term stability and conditions of storing to allow their actual application.

3. Electrochemical Biosensor Based on Catalysts

The catalysts including, enzymes, chemical catalysts, and DNAzyme have been used for miRNA detection (Figure 6). Enzymes are biomacromolecules with highly selective catalytic activities. More than 5000 biological processes have been established to be catalyzed by enzymes. Additionally, they can accelerate chemical reactions with tremendously high efficiency and selectivity, typically with 10^{10} – 10^{15} -fold rate enhancements over uncatalyzed chemical reactions.

Nanomaterials as chemical catalysts can also mimic enzyme catalysis by their ability to act in catalytic processes and are potentially viable alternatives for enzymes. Thus, they attract a great deal of interest and have been actively researched over decades. Indeed, nanomaterials have unique physico-chemical properties, including a size comparable with natural enzymes, a high surface/volume ratio, a large number of catalytically active sites on their surface, as well as the availability of multifunctional reactive groups for subsequent modification and functionalization. The high surface/volume ratio and a large number of active sites should result in a high catalytic efficiency [91].

DNAzymes are ssDNA molecules that also exhibit a catalytic activity and are exploited in biology, medicine, and material sciences. Development in this field is related to the many advantages of DNAzymes over conventional protein enzymes, like simpler preparation and thermal stability [92]. In this section, electrochemical biosensors for miRNA detection based on the enzymes, chemical catalysts, and DNAzyme will be discussed.

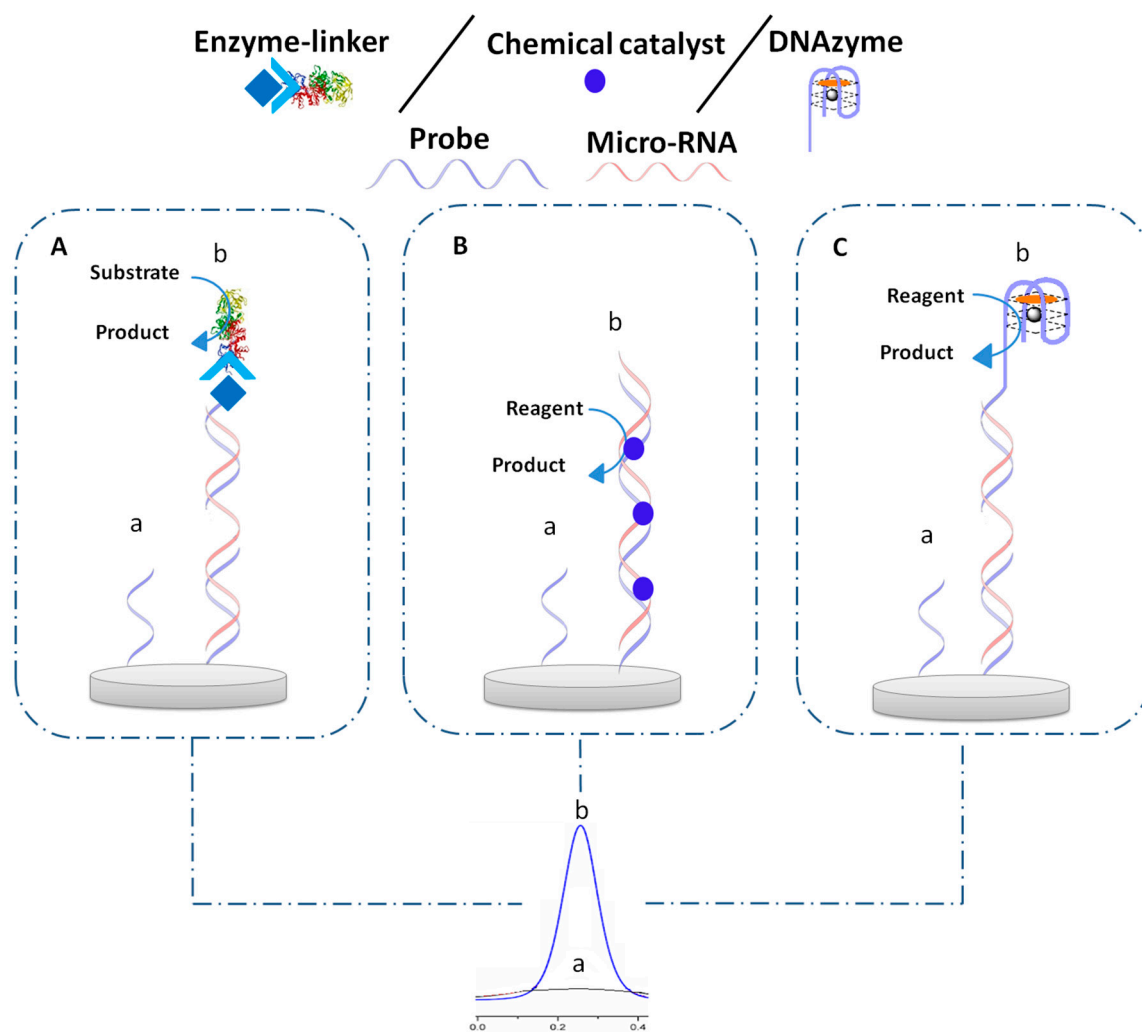


Figure 6. Principle of electrochemical biosensor based on different types of catalysts before (a) and after hybridization (b) with micro-RNA, (A) enzyme, (B) chemical catalyst, (C) DNAzyme.

3.1. Enzyme

The use of an enzyme in amplification strategies is widely used for miRNA detection. It includes various enzymes that lead to obtaining electroactive species which could be electrochemically detected. The most employed enzymes are alkaline phosphatase (ALP) and horseradish peroxidase (HRP). The binding strategy of the enzymes to the biosensors is the key to biosensors' success because it could affect the accessibility of the active site or lead to denaturation. In this regard, different works have been reported based on the different types of binding approach on the biosensor that will be discussed in this part. Some examples of enzyme binding approaches are presented in Figure 6A.

3.1.1. Enzyme–Streptavidin Binding

The binding of an enzyme on the biosensor via the interaction between biotin-modified probe sequence and streptavidin-modified enzyme is a habitually used method in the literature of enzyme binding employed for miRNA detection [93–96]. Using this type of interaction between a biotinylated capture probe and streptavidin-conjugated alkaline phosphatase (SA-ALP), Xia et al. [97] described an electrochemical–chemical–chemical (ECC) RedOx cycling system for miRNAs detection with Fc methanol, which acts as the RedOx mediator using TCEP as a reducing agent and L-ascorbic acid 2-phosphate as a substrate of ALP enzyme. With this system, one ALP enzyme captured by one target miRNA molecule favored the production of thousands of ascorbic acid (AA) enzymatic products,

which allowed a sensitive detection with an LOD of 40 fM. This biosensor could be generated 10 times, which permits an increase in the sample throughput and reduces the sample analysis time. In another work based also on the ECC system, a sandwich biosensor was employed using a biotinylated DNA-linked GO-AuNPs hybrid as a signal probe, which was interacted with SA-ALP. A capture probe was immobilized on GCE/AuNPs/Magnesium oxide (MgO) for more sensitive miRNA detection of 50 aM [98]. Mandli et al. [99] developed an electrochemical miRNA biosensor based also on a sandwich system with the use of AuNPs as a biosensor platform that incorporates SA-ALP enzyme linked to a biotin-modified signaling probe, catalyzing α -naphthyl phosphate as a substrate to produce electroactive α -naphthol. The differential pulse voltammetry (DPV) technique was used for the measurement of α -naphthol oxidation.

A competitive RNA/RNA hybridization assay-based biosensor was developed by incorporation of SA-HRP linked to biotinylated capture probes for amperometric detection of miRNA using H_2O_2 as enzyme-substrate and hydroquinone (HQ) as RedOx mediator. Indeed, different platforms—one based on the screen-printed electrode (SPE)/AuNPs [100] and the other one based on GCE/tungsten diselenide/AuNPs [101]—were employed. A lower LOD of 0.06 fM was obtained using tungsten diselenide/AuNPs because tungsten diselenide displayed a large effective surface area. This allowed increased loading of AuNPs on its surface to act as an excellent sensing substrate, which therefore can immobilize more capture probe DNA to the electrode and in turn leads to a low LOD.

Using a new way for probe capture immobilization, Torrente-Rodríguez et al. [102] employed magnetic-beads (MBs) modified with a special DNA–RNA antibody as capture probe bioreceptor. The antibody recognized the hybridized microRNA and biotinylated capture probe linked to SA-HRP. Indeed, amperometric detection implying the H_2O_2 /HQ system at disposable SPCE was performed. This methodology has been evaluated for the quantification of miRNA-205 and miRNA-21 in total RNA obtained from human breast tissues.

In another work, simultaneous detection of four miRNAs using DNA tetrahedral nanostructure-based sandwich-type assay and Poly-HRP40 was performed in a serum sample of pancreatic cancer patients. A biotinylated capture signaling probe linked to HRP-SA was hybridized with the immobilized DNA tetrahedral on the gold electrode surface. Indeed, the HRP enzyme catalyzed the reduction in H_2O_2 in the presence of microRNAs, with TMB employed as an electron mediator, and thus generated a quantitative amperometric signal in the presence of TMB substrate [103]. Despite, the advantages of simultaneous detection with the presented method, it is still unable to give a specific LOD of each analyzed miRNA because of the interaction of the enzyme with all of the biotinylated signal probe complementary sequences of each miRNA.

Enzyme reaction-based electrochemical biosensor-integrated hybridization chain reaction (HCR) amplification was used to enhance the sensitivity of detection. Using this method, a large amount of streptavidin enzyme binds to biotin labeled on the long-range HCR product, which could remarkably amplify electrochemical signals. Different electrochemical biosensor based HCR techniques and the interaction between biotin-modified probe sequence and streptavidin-modified enzyme were developed [104,105]. Indeed, Zhai et al. [104] developed an electrochemical biosensor based on HCR and ALP by measuring the oxidation of α -naphthol as the enzymatic product, which is proportional to the miRNA concentration, an LOD of 0.56 fM was obtained. This biosensor has a good stability of 2 weeks.

Otherwise, in other work, DSN was employed; indeed, biotinylated ssDNA capture probes were immobilized on gold electrodes allowing SA-ALP to be attached to the capture probe, facilitating the production of an electrochemically active p-aminophenol (p-AP) from p-aminophenyl phosphate (p-APP) substrate. The resulting p-AP was cycled by TCEP after its electro-oxidization, enabling an increase in the anodic current of p-AP, which is proportional to miRNA concentration. Due to the cleavage of the double-strand DNA (dsDNA) by DSN, a decrease in p-AP response was observed after hybridization indicating the presence of miRNA [106]. More sensitive biosensors were developed also using DSN and the introduction of nanomaterials as a biosensor platform. However, the detection of

miRNA was performed by the evaluation of AA using ALP and ECC RedOx cycling, using different platforms such as GCE/molybdenum disulfide (MoS_2)/AuNPs and GCE/MWCNTs@graphene oxide nanoribbons (GONRs)/AuNPs [107,108].

Other works for miRNA detection based on enzymatic reaction reported the use of CHA, which is initiated by the presence of target miRNA [109–112]. CHA allows the infinite recycling of miRNA to create a mass of streptavidin-enzyme modified signal probes, leading to an enhancement of electrochemical response. Additionally, to further enhance the sensitivity for miRNA detection, nanomaterials linked to enzymes were used. In this regard, Chen et al. [109] proposed a sandwich system integrating CHA and carbon sphere- MoS_2 (CS- MoS_2)/AuNPs for the immobilization of capture DNA (see Figure 7). AuNP-modified biotinylated signaling probes were employed as carriers of Avidin-HRP, which catalyze the $\text{H}_2\text{O}_2 + \text{HQ}$ system to produce a strong electrochemical response, used for sensitive miRNA detection, to achieve a lower LOD of 0.16 fM.

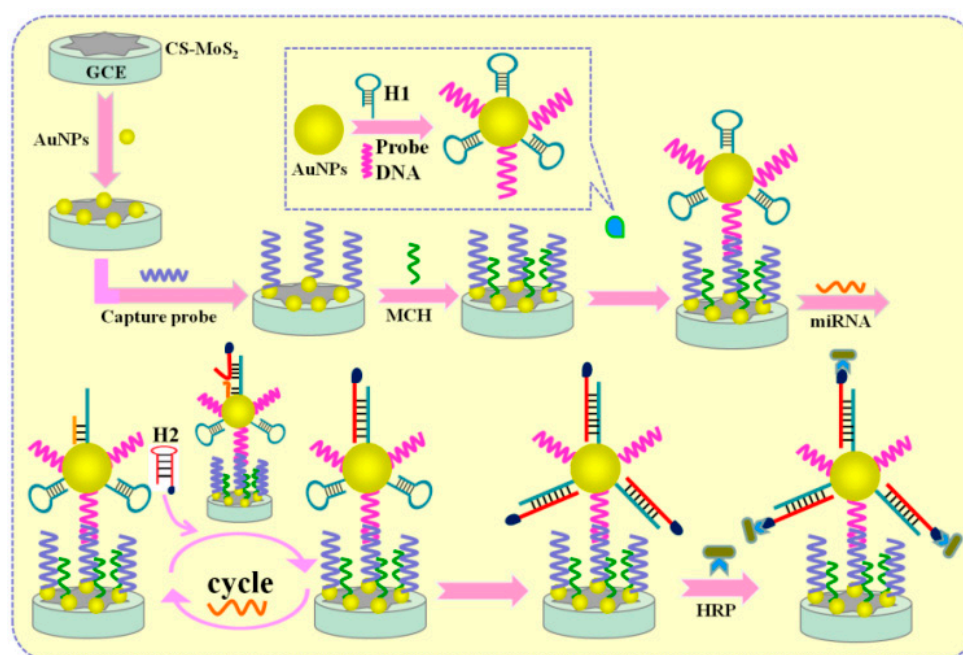


Figure 7. A sandwich-type electrochemical biosensing platform for microRNA-21 detection using carbon sphere- MoS_2 and catalyzed hairpin assembly for signal amplification (reproduced with permission from the publisher) [109].

Zhang et al. [113] used DSN for miRNA-21 detection coupled with a capture probe labeled with biotin and SA-coated AuNPs, which were immobilized on the electrode surface due to the SA/biotin interaction. The numerous SA-coated AuNPs can subsequently immobilize a large number of biotin-labeled HRP molecules. Indeed, AuNPs were used as nanocarriers for HRP, helping to maintain their enzymatic activity. HRP was used to catalyze the reduction in H_2O_2 and in the presence of TMB, electrochemical current signals can be generated, which considerably enhances the electrochemical signal for miRNA-21 detection. The proposed biosensor permits an LOD of miRNA-21 down to 43.3 aM. The proposed biosensor allows an analysis of miRNA-21 in the human lung cancer cell line (A549 cells).

3.1.2. Enzyme–Protein Binding

The immobilization of enzymes is also possible by a protein. In this regard, Fang et al. [114] reported an electrochemical biosensor based on the immobilization of enzyme HRPs through zinc finger protein, which binds preferably to the DNA–RNA hybrid formed between an ssDNA capture probe and a target miRNA-21. For sensitive detection, ECC was used as an amplifier system based on the induction

of a series of oxide-reduction reactions in the presence of HRP including $\text{Ru}(\text{NH}_3)_6^{3+}/\text{Ru}(\text{NH}_3)_6^{2+}$, BQ/HQ, and TCEP. The LOD for miRNA-21 in the buffer and diluted human serum were 2 and 30 fM, respectively.

Enzyme-conjugated protein was also employed for labeling an antibody that specifically recognizes DNA–RNA duplex [115]. In this view, Vargas et al. [116] involved the use of direct hybridization of miRNA-21 with a specific biotinylated DNA probe immobilized on streptavidin-modified MBs. A specific antibody labeled with a bacterial protein A conjugated with Poly-HRP40 recognized the capture probe/miRNA-21 duplex. Amperometric detection of miRNA-21 was performed upon the magnetic capture of the modified MBs onto the SPCEs using the $\text{H}_2\text{O}_2/\text{HQ}$ system.

Zouari et al. [117] developed an electrochemical AuNP-based biosensor platform that was used for miRNA detection. Indeed, RNA/miRNA homoduplexes were recognized with the viral protein p19, labeled with a HRP-conjugated anti-maltose binding protein monoclonal antibody (see Figure 8). The bioplatfroms present at least 2 months of storage stability. Additionally, the analysis of miRNA in total RNA extracted from healthy and cancerous breast cells was performed using the proposed biosensor.

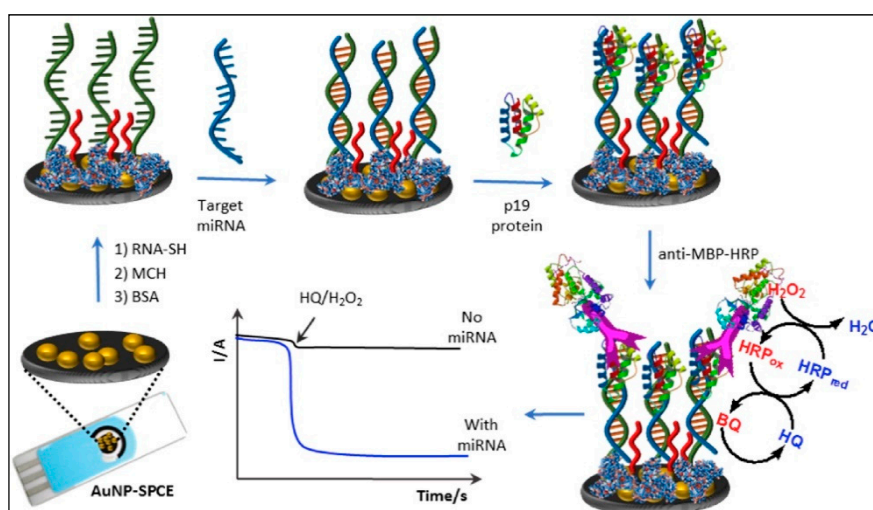


Figure 8. Schematic display of the amperometric integrated sensor developed for miRNA determination using a specific thiolated RNA probe, a direct RNA/miRNA hybridization assay and p19 viral protein as detector bioreceptor further labeled with anti-MBP-HRP (reproduced with permission from the publisher) [117].

3.1.3. Other Types of Enzyme Binding

There is another way for enzyme immobilization at the electrode surface for miRNA detection. Indeed, graphene quantum dots (GQDs) have a large surface-to-volume ratio, excellent compatibility of GQDs were used as a new platform for a large amount of HRP immobilization through the non-covalent assembly (see Figure 9). In this work, a sandwich system was employed for miRNA-155 detection integrating capture probe and signaling probe modified with NH_2 conjugated with QDs-HRP. The proposed biosensor is permitted to reach an LOD of 0.14 fM in a linear range from 1 fM to 100 pM [118]. Otherwise, an electrochemical biosensor for miRNA-221 detection using CHA and also a sandwich system based on the use of HRP directly labeled to signal probe was reported. HRP was used to catalyze the reaction of TMB/ H_2O_2 for amperometric detection of miRNA-221 [119].

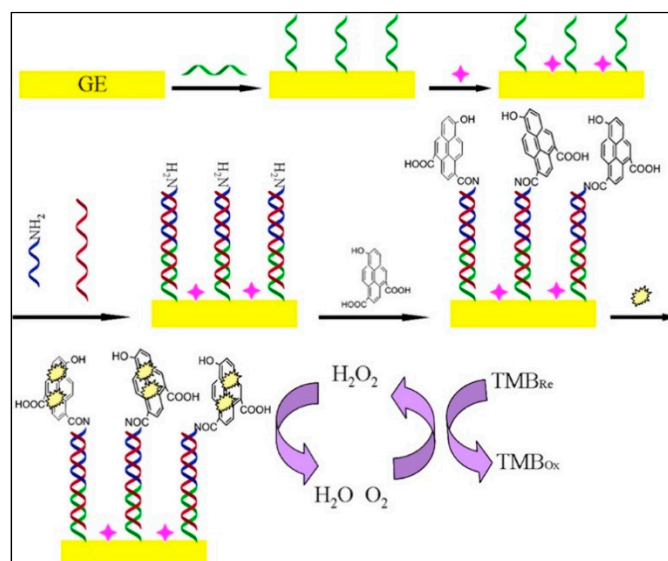


Figure 9. Principle of the enzyme catalytic amplification of miRNA-155 detection with graphene quantum dot-based electrochemical biosensor (reproduced with permission from the publisher) [118].

3.2. Chemical Catalysts

Different kinds of nanomaterials as chemical catalysts, including copper-based metal–organic framework (Cu-MOF), copper nanoclusters (CuNCs), Fe₃O₄NPs, platinum/tunable tin-doped indium oxide nanoparticles (Pt/Sn-In₂O₃) were utilized for miRNA detection and will be discussed in this part. An example of an electrochemical biosensor for miRNA detection based on the chemical catalyst is presented in Figure 6B.

Wang et al. [120] proposed a paper modified AuNP as a biosensor platform for miRNA-155 detection using a capture probe-AuNPs@Cu-MOF (see Figure 10). In the presence of glucose, Cu-MOFs and AuNPs as chemical catalysts cooperatively catalyzed the glucose oxidation, resulting in the wide linear detection range from 1.0 fM to 10 nM and the LOD of 0.35 fM for miRNA-155. The present biosensor showed stability of 30 days.

In other work, CuNCs as catalyst-based biosensor were employed for miRNA detection. CuNCs were synthesized at the electrode surface by taking DNA–RNA heteroduplexes as templates with the help of AA and Cu²⁺. Besides, the formed CuNCs possessed the capability of catalyzing H₂O₂ reduction, resulting in steady and amplified electrochemical signals, which were used in miRNA analysis, reaching an LOD of 8.2 fM [121]. As other types of nanomaterial as a chemical catalyst, SA/Pt/Sn-In₂O₃ hybrids were employed for miRNA-21 biosensor development. Indeed, a SA/Pt/Sn-In₂O₃ was attached to a biotinylated hairpin capture probe by the presence of miRNA-21, producing an electrochemical signal of oxygen reduction for detection in O₂-saturated solution. SA/Pt/Sn-In₂O₃ as the amplifier led to an LOD of 1.92 fM [122].

Otherwise, a mixing of enzyme and nanomaterial as enzyme–nanomaterials composite was reported to enhance the sensitivity for miRNA detection [123–126]. This is obtained by the synergetic effect of the catalyst and nanomaterials that improve the electrochemical response. However, the LOD of miRNAs obtained with this composite could be also obtained using just one type of catalyst; consequently, the use of enzyme and nanomaterials as catalysts together increases the cost and the time of biosensor construction without significant signal amplification.

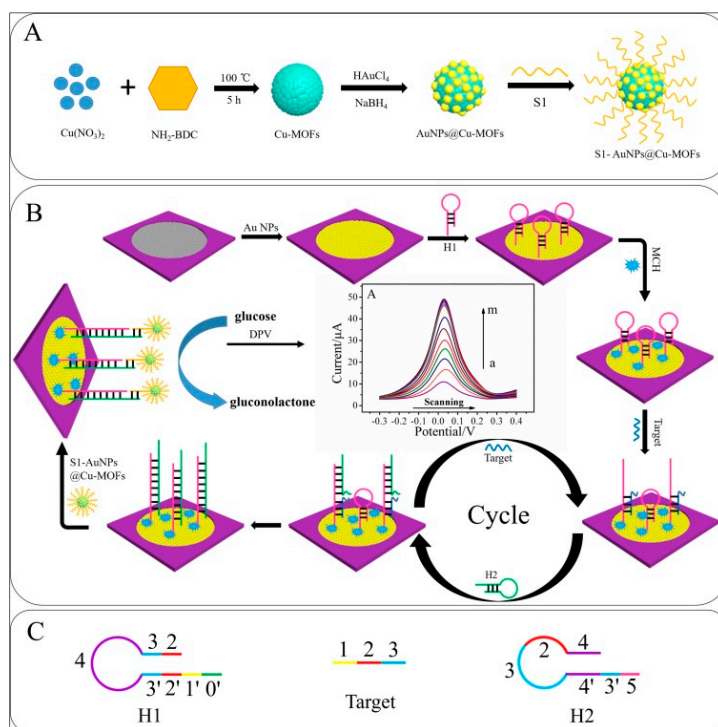


Figure 10. Schematic illustration of the fabrication of the biosensor: (A) preparation procedure of S1-AuNPs@Cu-MOFs; (B) the detection principle for glucose and the strategy of signal amplification; (C) structure of H1, target, and H2 (reproduced with permission from the publisher) [120].

3.3. DNAzyme

Recently, DNAzymes with peroxidase-like activity has aroused a high interest. To achieve such catalytic activity, the DNA probe requires a G-quadruplex structure, which is able to bind to hemin molecules. Such a system promotes a RedOx reaction between the target molecule and hydrogen peroxide, leading to the formation of an oxidized product. Indeed, hemin-G-quadruplex was employed for miRNA detection [127,128]. The principle of an electrochemical biosensor based on hemin-G-quadruplex as a DNAzyme is presented in Figure 6C. In this context, hemin-G-quadruplex was employed to catalyze H_2O_2 reduction, with coupling with HCR to fabricate long hemin-G-quadruplex DNAzyme nanowires (see Figure 11) [129]. In other work, hemin-G-quadruplex was also used for miRNA analysis by catalyzing the oxidation of TMB in the presence of H_2O_2 [130].

Table 3. Current sensitive electrochemical biosensors using catalysts.

MicroRNA	Catalysts/Amplification Agents	Platform	Substrat or Reagent	Technique	Linear Range	LOD	Real-Samples Application	References
miRNA-21	ALP/DNA-linked GO-AuNPs	GCE/MgO/AuNPs	AAP	DPV	0.1–100 fM	50 aM	Spiked human serum	[98]
miRNA -21	ALP/HCR	AuE	α -NP	SWV	1 fM–100 pM	0.56 fM	Spiked HEK293T cells	[104]
miRNA-21	ALP/CHA-WO ₃ -Gr	GCE/WO ₃ -Gr/AuNPs	Ascorbic acid 2-phosphate	DPV	0.1 fM–100 pM	0.05 fM	Serum samples from breast cancer patients	[111]
miRNA -21	HRP/AuNPs	AuE	H ₂ O ₂	Amperometry	0.1 fM–100 pM	43.3 aM	A549 tumor cells	[113]
miRNA-155	ALP/CHA	GCE/MWCNTs PtNPs	Phosphate ion Molybdophosphate anion	DPV	10 fM–1 nM	1.64 fM	Cervical cancer cells and human breast cancer cell lines	[131]
miRNA-155	ALP/-	SCPE/Fe ₃ O ₄	AAP	DPV	0.6–9 ng/mL	29 pM	Spiked human serum	[132]
miRNA-21	HRP/-	SCPE/Fe ₃ O ₄	H ₂ O ₂	Amperometry	1.0–100 pM	10 aM	MCF-7 cells	[116]
miRNA -155	HRP/GQDs	AuE	TMB	Amperometry	1 fM–00 pM	0.14 fM	Spiked human serum	[118]
miRNA-21, let-7a & miRNA-31	HRP/HCR	SPCE/Fe ₃ O ₄	H ₂ O ₂	Amperometry	1.2–100 pM	0.66 pM	MCF-7 cells	[133]
miRNA-21	HRP/-	SPCE/Fe ₃ O ₄	H ₂ O ₂	Amperometry	3.0 to 100 nM	0.91 nM	MCF-7 cells	[134]
miRNA-21	Copper (II) complex/HCR	GCME/Fe ₃ O ₄	TMB	DPV	100 aM–100 nM	33 aM	human serum samples from breast cancer	[135]
miRNA-155	Cu-MOFs/AuNPs	Au-PWE	Glucose	DPV	1 fM–10 nM	0.35 fM	Spiked human serum	[120]

Table 3. Cont.

MicroRNA	Catalysts/Amplification Agents	Platform	Substrat or Reagent	Technique	Linear Range	LOD	Real-Samples Application	References
miRNA-21	Sn-In ₂ O ₃ /-	AuE	O ₂	DPV	5 pM–0.5 fM	1.92 fM	A549 and HeLa cell lines	[122]
miRNA-21	G-quadruplex–hemin/-	AuE	H ₂ O ₂	DPV	0.1 fM–0.1 pM	0.04 fM	Human serum samples from breast cancer	[128]
miRNA-21	G-quadruplex–hemin/HCR	AuE/SWCNT-ox/NDs/SWCNTs-ox/AuNPs	H ₂ O ₂	DPV	10 fM–1.0 nM	1.95 fM	Spiked human serum	[129]

Abbreviations: GCE, glassy carbone electrode; NDs, nanodiamonds; MB, magnetic beads; SWCNTs, single-walled carbon nanotubes; α -NP, α -naphtyl phosphate; AAP, ascorbic acid 2-phosphate; WO₃-Gr, tungsten oxide-graphene composites; AA, ascorbic acid; ALP, alkaline phosphatase; CHA, catalytic hairpin assembly; DPV, differential pulse voltammetry; MgO, magnesium oxide; GO, graphene oxide, AuNPs, gold nanoparticles; AuE, gold electrode; HCR, hybridization chain reaction; SWV, square wave voltammetry; HEK293T cells, from human embryonic kidney 293T cells; SPCE, screen-printed carbon electrodes; H₂O₂, hydrogen peroxide; HRP, horseradish peroxidase; MCF-7 cells, human breast adenocarcinoma cell line; TMB, 3,3',5,5'-tetramethylbenzidine; GQDs, graphene quantum dots; A549, human lung carcinoma cells; HeLa cells, human cervical cancer cells; Au-PWE, gold-paper working electrode; Cu-MOFs, copper-based metal–organic frameworks; G-quadruplex–hemin, Guanine-quadruplex–hemin; MDA-MB-231, human breast cancer cell lines, Sn-In₂O₃, tin-doped indium oxide particles. MWCNTs, multi-walled carbon nanotube, platinum nanoparticles, PtNPs; magnetic nanoparticles, Fe₃O₄.

4. Electrochemical Biosensor Based on RedOx Intercalating Agent

In chemistry, intercalation is the insertion of a molecule (or a group of molecules) between two other molecules (or groups). In the present approach, a RedOx molecule or a complex of RedOx molecules are employed for DNA strand binding via intercalation. The binding to ssDNA and dsDNA is obtained with different affinity regarding the nature of the intercalator. Different types of molecules were used as RedOx intercalating agents for miRNA analysis. This includes organic molecules such as the commonly used MB [136] as well as oracet blue (OB) [137] and toluidine blue [138]. Various other molecules and macromolecules could also be intercalated as an organometallic complex including $\text{Ru}(\text{NH}_3)_6^{3+}$ [139], cobalt phenanthroline, or metal intercalating agents such as palladium nanoparticles [140] and biomolecules as hemin [141]. The principle of the approaches is presented in Figure 12. The interlacing process on the biosensor could be direct to the target DNA strands (Figure 12A) [138] or indirect by the design of specific sites in the DNA probe called a template [142] (Figure 12B).

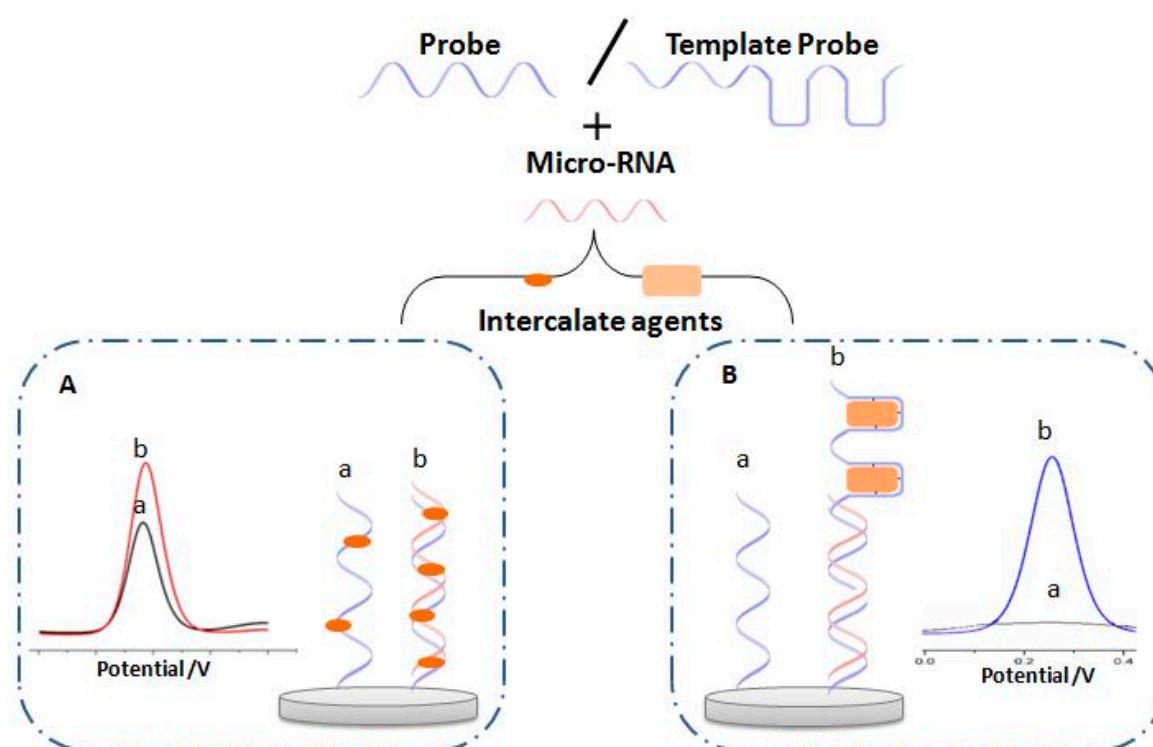


Figure 12. Principal of electrochemical biosensor based on RedOx intercalating agent before (a) and after hybridization (b) with micro-RNA, (A) direct intercalation, and (B) intercalation via the template.

4.1. Direct Intercalation

The direct intercalating of RedOx molecules between the DNA strands is based on an interaction of electroactive species on the formed double-strand DNA–DNA or DNA–RNA upon hybridization reaction (Figure 12A). Indeed, various kinds of RedOx molecules could be used in the case of electrochemical biosensors for miRNA that will be discussed in this part and they are divided into three kinds, electroactive molecules, and electroactive complex.

4.1.1. Electroactive Molecule

The MB is the popular electroactive indicator used as an intercalating DNA agent since MB interacts both with ss and ds DNA where the binding mode differs from each macromolecule. Thus MB and dsDNA interact by three binding modes: (i) intercalation between successive base pairs with the face-to-face binding of the bases and MB; (ii) insertion into the minor groove; and (iii) insertion into the

major groove of the double helix. The interaction ssDNA with MB is obtained by face-to-face binding of the bases and MB. Thus, the affinity of MB regarding ssDNA and dsDNA is largely discussed. Regarding the literature, depending on the biosensors design, MB shows a higher affinity for ssDNA or dsDNA. In the case of miRNA detection, most biosensors published show less affinity of MB to DNA–RNA complex. Thus, it has been reported by Li et al. [143] that MB reacts easily with guanine present in ssDNA with high affinity due to the good accessibility of MB to the guanine of ssDNA. In this work, a transducer formed with GCE/MWCNTs/PAMAM modified with a DNA probe was used as a biosensors platform for miRNA-24 detection. The detection was followed through measuring the electroactivity of MB before and after hybridization. A decrease in the signal response is observed after the hybridization of miRNA-24 where LOD reached 0.5 fM. Furthermore, this biosensor was stable for 7 days and could be regenerated four times.

Nevertheless, a more complex biosensor design was performed using RedOx intercalator and amplification strategy in order to enhance the sensitivity of the detection. For example, a biosensor was developed for miRNA-155 detection, where HCR was used to amplify the number of intercalated MB molecules on the DNA strands, by creating a longer dsDNA and using a GCE modified with polypyrrole/reduced graphene oxide/AuNPs (Ppy/rGO/AuNPs) [144]. The amplification of MB response can also be performed by using a 3D DNA nanonet structure which is hybridized with the immobilized capture probe on a gold electrode by a sandwich system. In this case, a femtomolar detection of miRNA-21, was obtained [145]. Both presented biosensors were stable for 2 weeks and the analysis of miRNA was performed in spiked human serum.

Another approach involving nanomaterials as nanocatalysts which assisted the signal amplification strategy has been used to enhance the RedOx signal of MB intercalator. For example, the association of various kinds of nanomaterials as a catalyst was developed to improve the MB response. Thus, the synergetic effect of Fe₃O₄ and cerium dioxide (CeO₂) decorated with gold nanoparticles (Fe₃O₄/CeO₂@AuNPs) was demonstrated to improve the RedOx response of MB intercalator (Figure 13A). A labeled probe decorated with the nanocatalysts was employed in a sandwich system for the amplification of intercalated MB response by a direct catalyzation of MB reduction leading to LOD of 0.33fM [146]. Other nanomaterials such as carboxylate-reduced graphene oxide (COOH-rGO) have been reported as an amplification strategy. The nanomaterial can intercalate on the ssDNA, leading to an accumulation of electroactive MB (Figure 13B). In the presence of miRNA, a DSN cleave captures probe/miRNA duplex is obtained resulting in a decrease in MB response. A lower LOD of 0.01 fM was obtained [147].

Other approaches involving various innovative amplification strategies have also been published. For example, Guo et al. [148] reported an attomolar biosensor for the detection of miRNA-196a. The mechanism consists of after hybridization of miRNA and formation of a terminal deoxynucleotidyl transferase will trigger a DNA extension reaction producing long ssDNA rich in guanine, in which MB is attached. The biosensor presents a very low sensitivity compared to other ones, used with other strategies due to obtained long ssDNA which can specifically adsorb positively charged MB via guanine bases, resulting in the attachment of a large amount of MB. However, this biosensor needs many steps after miRNA hybridization which can limit their application.

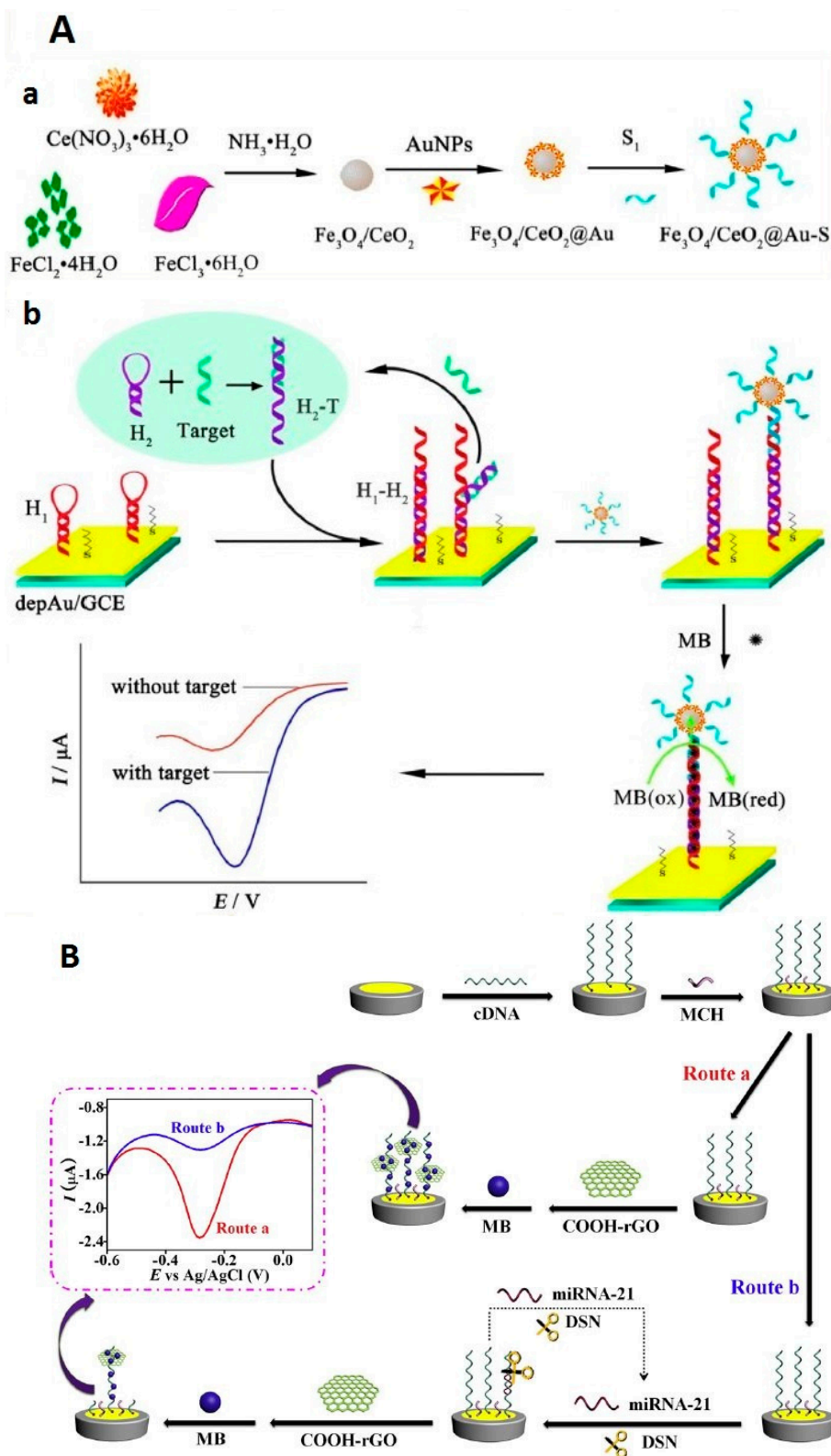


Figure 13. Example of biosensors using amplification strategy with nanomaterials as a non-nanocatalyst; (A) the nanomaterials are formed with Fe_3O_4 and cerium dioxide (CeO_2) decorated with gold nanoparticles ($Fe_3O_4/CeO_2@AuNPs$) reproduced from. (a) Preparation procedure of $Fe_3O_4/CeO_2@Au-S_1$, (b) signal amplification strategy and the detection principle for microRNA [146] with permission of the publisher; (B) biosensors using graphene oxide and DSN as amplification method from [147] reproduced with permission of the publisher.

4.1.2. Electroactive Metals Complex

In the case of electroactive metal complex intercalator, hexaammineruthenium III chloride (RuHex) is used frequently as electroactive complex employed for miRNA detection. The RuHex is positively charged and could intercalate with DNA strand via the binding with the anionic phosphate of DNA through electrostatic interaction. Few studies have been published with this complex and the associated amplification strategies. For example, hierarchical flower-like gold nanostructures (HFGN) were developed as a biosensor platform and used for selective detection of miRNA-21 in the buffer and real sample; RuHex was employed as RedOx intercalator [149]. In other works and to increase the amount of intercalated RuHex, Yu et al. [150] and Chen et al. [151] used DNA nanostructures as probes immobilized on the gold electrode surface for enhancing the binding ability of RuHex. Thus, in the presence of miRNAs targets, these nanostructures provided an enhancement of RuHex intercalants. The analysis of miRNA in total RNA-extracted cancerous breast cells was performed using the proposed biosensors.

4.2. Intercalation via Template

The intercalation via template consists of the use of other molecules, which need to create recognition sites in DNA strands for their intercalation. The principal of this type of intercalation is presented in Figure 12B. Generally, the nanostructure of DNA is necessary to perform this method.

Starting with hemin that needs abundant guanines to form hemin/G-quadruplexes [152], an electrochemical biosensor was described by Wang et al. [153] for the quantification of miRNA-21 at fM level. The catching of hemin was enhanced by the integration of a sandwich system in which a signal probe is labeled with N-doped graphene/Au nanoparticles (NG-AuNPs) and works as a support for several strands of guanine-rich DNA.

Otherwise, Zhang et al. [140] described a label-free and attomolar electrochemical miRNA-21 biosensor based on a template for palladium nanoparticles which lead to integration with the nitrogen of guanine. RCA amplification was used to produce a massive G-rich long ssDNA resulting in an enhanced electrochemical signal.

4.3. Other Type of Intercalation

Some other RedOx molecules able to intercalate poorly or that do not intercalate at all with the DNA strands have also been studied. However, their intercalation could be realized via a linker. In this regard, Asadzadeh et al. [154] used AgNPs as a RedOx molecule, which was intercalated to the ssDNA via single-walled carbon nanotube (SWCNT). The binding of the AgNPs/SWCNT nanohybrid to ssDNA was performed via interactions π - π between the nanohybrid and the nitrogenous bases of ssDNA. The proposed method was used for miRNA-25 detection as a lung cancer biomarker.

Wang et al. [155] used GO as support of Prussian blue (PB), which is the RedOx intercalant agent. The GO was adsorbed on the 3' end of capture probe through π - π interaction. Then, the PB was attached to GO. In the presence of miRNA-122, the GO with the assembled PB was separated from the electrode surface due to the low affinity of the GO with the DNA/RNA hybrid, resulting in a decrease in electrochemical response of PB.

MiRNAs are characterized by cis-diol at the 3'-terminal, this propriety is employed by Liu et al. [156] for an attomolar detection of miRNA-21 using AgNP as a RedOx intercalate agent. Indeed, with the presence of miRNA-21, a 4-mercaptophenylboronic acid (MPBA) was attached in the 3'-terminal of miRNAs through the boronate ester bond formation and then captured AgNP via the Ag-Thiol interaction. Meanwhile, free MPBA molecules in solution induced the in situ assemblies of AgNPs on the electrode surface via the covalent interactions between α -hydroxycarboxylate of citrate and boronate of MPBA and the formation of Ag-Thiol bonds.

Electrochemical biosensors based on RedOx intercalating agents highlighting their various analytical performances are presented in Table 4.

Table 4. Current sensitive electrochemical biosensors using the RedOx intercalating agent.

MicroRNA	Intercalant Agent	Platform	Amplification of Signal Elements	Tech	Linear Range	LOD	Real-Samples Application	Ref
miRNA-155	OB	GCE/GO/GNR	-	DPV	2.0 fM–8.0 pM	0.6 fM	Spiked human plasma	[157]
miRNA-21	TB	GCE/AuNPs-Ppy	-	DPV	100 aM–1 nM	78 aM	Spiked human serum.	[138]
miRNA-196a	MB	AuE	DNA extension reaction	DPV	0.05 fM–50 pM	15 aM	Spiked plasma	[148]
miRNA-486-5p	Thinonine	GCE/FeCN/AuNPs	FeCN	DPV	1 fM–1000 pM	8.53 fM	Human lung A549 cells	[158]
miRNA-141	RuHex	AuE	HP-AuNPs	DPV	0–10 nM	25.1 aM	Human breast cancer cells MDA-MB-231	[150]
miRNA-21	RuHex	AuE	AuNPs enrichment by bridge DNA,	Chronocoulometry	0.1 fM–0.1 nM	68 aM	Serum samples from lung cancer patients	[159]
miRNA-21	RuHex	GCE/AuNPs@MoS ₂	AuNPs@MoS ₂	DPV	10 fM–1 nM	0.78 fM	Spiked human serum	[160]
miRNA-21	Molybdophosphate	AuE	HCR	SWV	1 fM–1 nM	0.78 fM	Spiked human serum	[161]
miRNA-21	CuNCs	AuE	HCR	DPSV	10 pM–0.1 fM	10 aM	Spiked blood sample	[162]
miRNA-21	Hemin	AuE	HCR	DPV	15 fM–250 pM	13.5 fM	Spiked human serum	[152]
miRNA-199 a	AgNPs	AuE	C-rich loop DNA templates	DPV	1.0 fM–0.1 nM	0.64 fM	Spiked human serum	[142]

Abbreviations: GCE, glassy carbon electrode; MB, methylene blue; DPV, differential pulse voltammetry; AuE, gold electrode; FeCN, iron-embedded nitrogen-rich carbon nanotubes; AuNPs, gold nanoparticles; A549 cells, adenocarcinoma cells; GO, graphene oxide; GNR, gold nanorods; Ppy, polypyrrole; RuHex, hexaammineruthenium III chloride; HP-AuNPs, hairpin-modified gold nanoparticles; MDA-MB-231: human breast cancer cells; HCR, hybridization chain reaction; SWV, square wave voltammetry; CuNCs, copper nanoclosters; DPSV, differential pulse stripping voltammetry; AgNPs, silver nanoparticles; C-rich loop DNA templates, cytosine-rich loop DNA templates; TB, toluidine blue; OB, oracet blue.

A comparison between different methods of intercalation used for miRNA detection shows that intercalation via a template presents some advantages such as good biocompatibility, good electrochemical properties facilitating a very low LOD of miRNA detection. Nevertheless, it still presents some limitations related to the complicated process of fabrication, which is considered time-consuming; and also, the need for an additional amplification step to obtain high sensitivity which is required for miRNA detection. Otherwise, direct intercalation of the RedOx molecules method is considered as an easy and fast method of intercalation since the used RedOx molecules could bind directly and specifically to DNA without the need of complicated preparation. Indeed, the LOD obtained using this method is slightly higher than the ones obtained with intercalation via the template method.

Overall, the intercalation strategy is easy to use on-site, but it does not allow simultaneous detection, because the interaction of the RedOx molecule is not specific and can intercalate on all DNA strands present at the surface of the electrode. Furthermore, the use of intercalation based on electrostatic interaction leads to a non-specific interaction and high background noise, especially using real samples.

5. Electrochemical Label-Free Biosensing

Label-free biosensor include the use of ferri-ferrocyanide complex or hexaammineruthenium (II)/(III) as RedOx-free indicators. The response is based on electrostatic repulsion or interaction depending on the marker. The ferri-ferrocyanide complex is negatively charged, thus after the hybridization of miRNA target, a repulsion effect is produced by the negatively charged phosphate leading to the variation of response. In the case of hexaammineruthenium (II)/(III) complex, it is positively charged and could undergo interaction with hybridized DNA. Another factor that could lead to the variation of the RedOx marker is its accessibility to the surface after DNA-RNA complex formation of a duplex preventing electron transfer to the surface. Various electrochemical methods could be used to follow such responses including electrochemical impedance spectroscopy (EIS), cyclic voltammetry (CV), DPV, and square wave voltammetry (SWV). The principle of electrochemical biosensors based on the free RedOx indicator is presented in Figure 14. In this section, electrochemical biosensors for miRNA detection based on the free RedOx indicator will be discussed.

5.1. Ferri/Ferrocyanide as Free RedOx Indicator

Ferri-ferrocyanide as a free RedOx indicator was widely employed for miRNA detection. The detection is based on the electrostatic repulsion of two negatively charged DNA and $\text{Fe}(\text{CN})_6^{3-/4-}$ molecules leading to the decrease in electrochemical reaction on the surface upon hybridization and decrease in current response or increase in impedance (Figure 14). In this regard, EIS as the detection method has been used extensively for miRNA monitoring in combination with various materials and nanomaterials as transducers [163–166]. In most research, the nature of materials attached to the surface plays an important role in the electrochemical response. In this respect, Yammouri et al. [167] used this approach in the association of transducer formed with a pencil graphite electrode (PGE) modified with a carbon black-bearing DNA probe. The miRNA-125a detection was monitored by EIS in the presence of this RedOx marker. The synergetic effect of negatively charged carbon black combined with the high surface ratio of PGE allows the detection with lower LOD and good determination in serum samples. In another work, the polythiophene film-modified screen-printed gold electrode was employed as a biosensor platform for miRNA-221 detection from total RNA extracted from human lung and breast cancer cell lines. The proposed biosensor demonstrated the benefic effect of the conductive surface [168]. Mandli et al. [169] employed PGE modified with Ppy for microRNA-34a detection by EIS. Indeed, the immobilization of the probe was performed during Ppy electropolymerization on PGE and the hybridization was performed by the specific recognition sequence of miRNA-34a. This biosensor was functional for the analysis of miRNA-34a in human breast cancer cells samples.

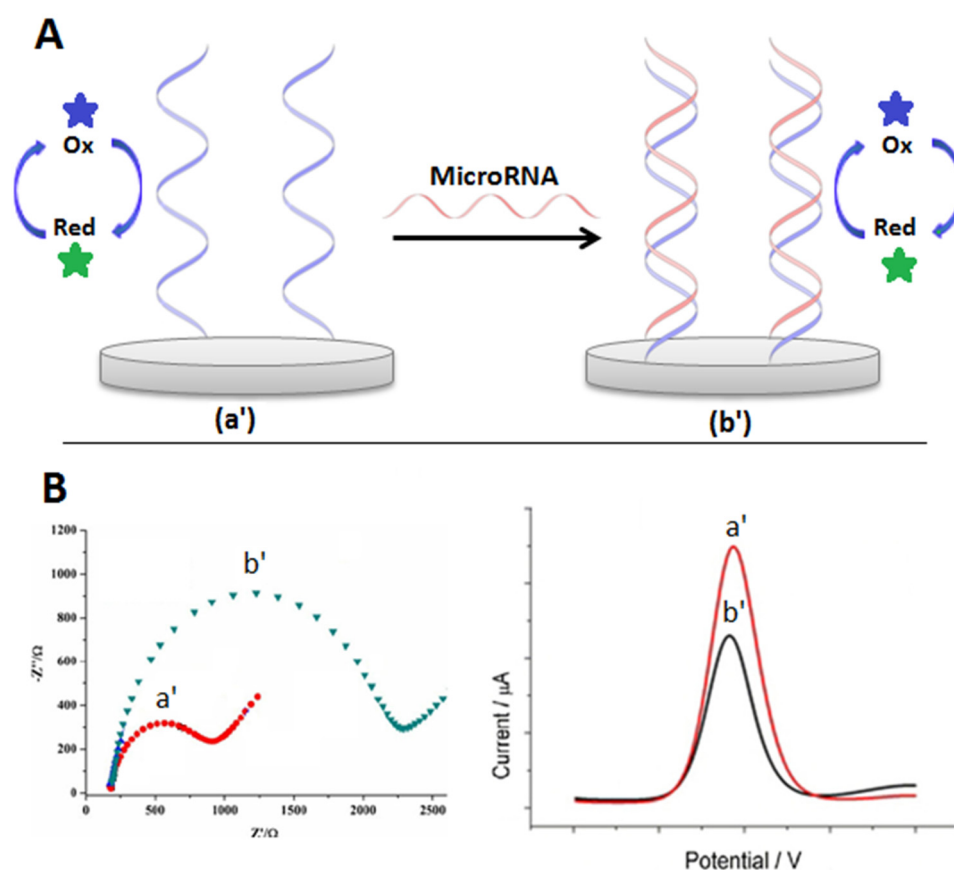


Figure 14. (A) Principle of electrochemical biosensors based on free RedOx indicator (a') before and (b') after hybridization. (B) EIS and DPV response of the electrochemical biosensor based on free RedOx indicator (a') before and (b') after hybridization.

Association of this method with system amplification such as HCR was also performed. Indeed, Meng et al. [170] developed an electrochemical biosensor combining efficient HCR for signal amplification of oligonucleotides with negatively charged repelling $[\text{Fe}(\text{CN})_6]^{3-/4-}$ ions inducing a spatial blockage to the electron transfer. In this biosensor, many linear DNA concatamers lead to a great increase in interfacial charge-transfer resistance (R_{ct}), which is positively correlated with miRNA-21 concentrations with an LOD of 4.63 fM with the stability of the biosensor lasting for 21 days. This strategy allowed the analysis of miRNA-21 in different cancer cells including breast, cervical, and non-small cell lung cancers.

Zhang et al. [171] employed a magnetic bead-modified glassy carbon electrode combined with a DSN amplification strategy for impedimetric miRNA-21 detection (see Figure 15). Due to the cleavage of the capture probe–miRNA-21 heteroduplex, after the hybridization steps the negatively charged layer could not be formed, resulting in a small R_{ct} in the presence of ferriferrocyanide, which was used for miRNA-21 detection, permitting an LOD of 60 aM.

Otherwise, DPV based on ferriferrocyanide was also employed for miRNA detection [172–174]. In this case, advanced surface modification was performed to obtain an efficient electron transfer. Indeed, a biosensor formed with fluorine-doped tin oxide electrode modified with nanomaterials composed with nitrogen-doped functionalized graphene associated with (AgNPs and polyaniline (PANI) nanocomposite modified, was developed for miRNA detection. The employed nanocomposite allowed more biomolecules to be immobilized at the surface of the electrode, which shortened the distance for electron transfer and ion diffusion paths from the capture probe to the nanomaterials. The nano-biosensor showed a wide dynamic detection range of 10 fM–10 μM and a low LOD of 0.2 fM [175].

Ferrirocyanide as a free RedOx indicator was used for other strategies of detection based on the direct adsorption of miRNAs on the electrode surface. This strategy needs a preliminary step of target isolation mostly with capture probe-modified magnetic beads, then, a denaturation of the DNA–RNA hybrid is achieved by heating at 95 °C. Thereafter, researchers try different ways for adsorbing isolated miRNAs. For instance, a picomolar biosensor was reported by Boriachek's group based on gold electrode–miRNA affinity interaction [176]. Wan's group used a screen-printed graphene electrode, for miRNAs detection isolated and directly adsorbed on the surface of the graphene electrode via graphene–miRNA affinity interaction. This method showed an LOD of 10 fM [177]. According to the present two works, we can conclude that graphene–miRNA affinity is higher than the gold–miRNA affinity. Koo et al. [178] magnified the adsorption of miRNAs using a polyadenine extension, which has a high affinity with the gold surface. However, the miRNA was subjected to poly (A) extension on 3' ends using poly(A) polymerase enzyme.

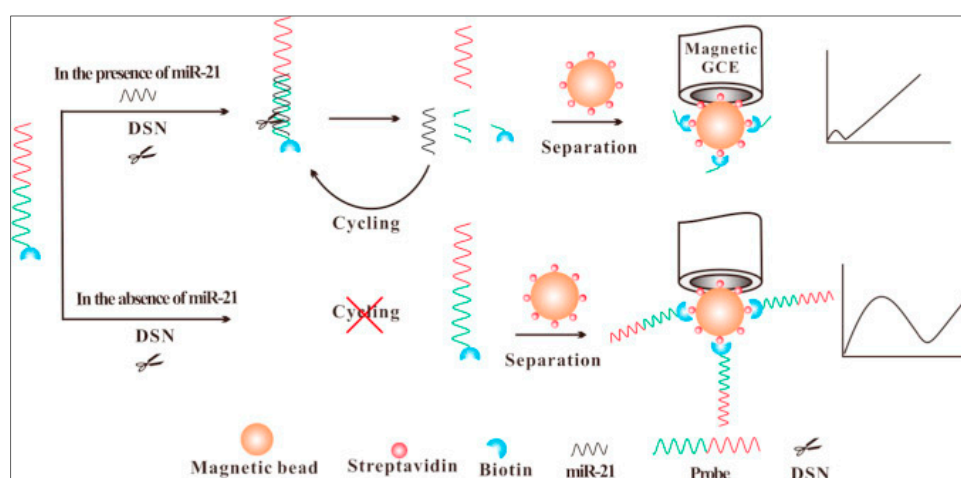


Figure 15. Experimental principle of the biosensor (reproduced with permission from the publisher) [171].

5.2. Hexaammineruthenium (II)/(III) Chloride as Free RedOx Indicator

Hexaammineruthenium (II)/(III) was also employed for miRNA detection. In this regard, nickel phosphate nanostructures (NiPNs) were used as a biosensor platform for the immobilization of the capture probe by coordination bonding between Ni and probe DNA especially phosphate groups. The constructed NiPNs-p-DNA surface acted as the amplified platform enabling efficient access to many target miRNA-21 sequences. The probe-DNA immobilization and the miRNA hybridization steps were supervised by EIS measurements in $[\text{Ru}(\text{NH}_3)_6]^{3+/2+}$. The proposed biosensor allowed reaching an LOD of 0.034 pM, and the analysis of miRNA-21 levels in human lung cancer cells [179].

Association of the two RedOx indicators ferricyanide and hexaammineruthenium (II)/(III) for miRNA detection was also explored. In this view, a ratiometric electrochemical miRNA biosensing platform based on the target-triggered ruthenium release and RedOx recycling was reported (see Figure 16). In this research, $[\text{Ru}(\text{NH}_3)_6]^{3+}$ was entrapped into the pores of mesoporous silica nanoparticles modified by an indium tin oxide electrode and was subsequently capped by a capture probe. Once the target miRNA was captured and hybridized into dsDNA/RNA, $[\text{Ru}(\text{NH}_3)_6]^{3+}$ was released and electroreduced into $[\text{Ru}(\text{NH}_3)_6]^{2+}$, which was then chemically oxidized back to $[\text{Ru}(\text{NH}_3)_6]^{3+}$ by $[\text{Fe}(\text{CN})_6]^{3-}$. The consumed $[\text{Fe}(\text{CN})_6]^{3-}$ and liberated $[\text{Ru}(\text{NH}_3)_6]^{3+}$ produced a significant ratiometric signal. Using this innovative approach, an LOD that decreased down to 33 aM was obtained. Additionally, the developed biosensor showed good stability over 20 days and permitted the analysis of miRNA-21 in different cancer cells including breast, cervical, and non-small cell lung cancers [180].

Electrochemical biosensors based on free RedOx indicator with the focus on their various analytical performances are exposed in Table 5.

The discussed methods in this section present some advantages including, higher sensitivity, easier signal quantification, direct conversion of the biological event into an electrical signal, and finally requiring fewer steps of fabrication since there is no need to use RedOx markers that interact with DNA strands. On the other hand, the inconvenience is that these methods suffer from some drawbacks such as the potential of non-specific adsorption of other biomolecules on the electrode surface, which may cause false-positive interference. Additionally, the results of this method were always easily disturbed by surface contamination and adsorption.

Table 5. Current sensitive electrochemical biosensors using free RedOx indicator.

MicroRNA	Free RedOx Indicator	Platform	Amplification Agent	Technique	Linear Range/LOD	LOD	Real-Samples Application	References
miRNA-21	Fe(CN) ₆ ^{3-/4-}	AuE	biotin-FNPs	EIS	0.1–250 fM	0.1 fM	-	[181]
miRNA-21	Fe(CN) ₆ ^{3-/4-}	GCE	AuNPs	EIS	1–1000 pM	0.3 pM	Spiked serum sample	[182]
miRNA-21	Fe(CN) ₆ ^{3-/4-}	Magnetic GCE	DSN	EIS	-	60 aM	Human serum from breast cancer patients	[171]
miRNA-199a-5p	Fe(CN) ₆ ^{3-/4-}	GCE/GO/GNR	GO and GNR	EIS	148 pM–15 fM	4.5 fM	Spiked human blood serum	[164]
miRNA-155	Fe(CN) ₆ ^{3-/4-}	Pt wire/Ti ₃ C ₂ Tx@FePcQDs	Ti ₃ C ₂ Tx@FePcQDs	EIS	0.01 fM–10 pM	4.3 aM	Spiked human serum samples	[165]
miRNA-21	Fe(CN) ₆ ^{3-/4-}	AuE	HCR	EIS	10 fM–50 pM	4.63 fM	A549, HeLa, MCF-7, RAW 264.7, and HUVEC cancer cells	[170]
miRNA-21	Fe(CN) ₆ ^{3-/4-}	SPE/rGO-Au	-	DPV	1 μM–1 pM	1 pM	Spiked artificial saliva	[183]
miRNA-319a	Fe(CN) ₆ ^{3-/4-}	GCE/AuNPs	nuclease S1	DPV	1000–5 pM	1.8 pM	-	[184]
miRNA-21	Fe(CN) ₆ ^{3-/4-}	FTO/NFG/AgNPs/PANI	-	DPV	10 fM–10 μM	0.2 fM	Spiked blood samples	[175]
miRNA-21	Fe(CN) ₆ ^{3-/4-}	FTO/CGO/Au-PtBNPs/SA	-	DPV	1 fM–1 μM	1 fM	spiked human serum	[174]
miRNA-21	Fe(CN) ₆ ^{3-/4-}	GCE/MWCNTs	TRNEAS	DPV	0.1 fM–5 pM	56.7 aM	MDA-MB-231, MCF-7, HeLa, and L02 cell	[173]
hsa-miR-486-5p	Fe(CN) ₆ ^{3-/4-}	Laser induced graphene	-	DPV	-	10 fM	-	[177]
miRNA-375	Fe(CN) ₆ ^{3-/4-}	AuE	-	SWV	10–30 fM	11.7 aM	CaP cells (PC-3, DU145, and LNCaP)	[185]
miRNA	[Ru(NH ₃) ₆] ^{3+/2+}	GCE/Ni PFNs	-	EIS	0.1–2500 pM	0.034 pM	A549 cancer cells	[179]
let-7a	[Ru(NH ₃) ₆] ^{3+/2+}	GCE/CNTs	CNT based solid-phase RCA	DPV	-	1.2 fM	HeLa cells	[186]
miRNA-21	Fe(CN) ₆ ^{3-/4-} /[Ru(NH ₃) ₆] ^{3+/2+}	ITO	-	DPV	0.1–1500 fM	33 aM	HeLa, A549, MCF-7 cancer cells	[180]

Abbreviations: HCR, hybridization chain reaction; FTO, fluorine-doped tin oxide; NFG, nitrogen-doped functionalized graphene; AgNPs, silver nanoparticles; PANI, polyaniline; CGO, carboxylated graphene oxide; Au-PtBNPs, gold platinum bimetallic nanoparticles; SA, streptavidine; GCE, glassy carbon electrode; MWCNTs, multi-walled-carbone nanotube; AuE, gold electrode; MGCE, magnetic glassy carbon electrode; GO, graphene oxide; Fe(CN)₆^{3-/4-}, ferri/ferrocyanide; DPV, differential pulse voltammetry; MDA-MB-231, human breast cancer cell lines; MCF-7, human breast adenocarcinoma cell line; HeLa, human cervical cancer cell line; and L02 cell; SWV, square wave voltammetry; DSN, duplex-specific nuclease; EIS, electrochemical impedance spectroscopy; GNR, gold nanoroad; Pt wire/Ti₃C₂Tx@FePcQDs, platinumium wire/iron phthalocyanine quantum dots; HUVEC, human umbilical vein endothelial; A549, non-small cell lung; RAW 264.7, mouse leukemia cells of monocyte-macrophage; biotin-FNPs, biotine-phenylalanine nanoparticles; Ni PFNs, nickel phosphate nanostructures; [Ru(NH₃)₆]^{3+/2+}, hexaammineruthenium(III) chloride; TRNEAS, target-recycled non-enzymatic amplification strategy; ITO, indium tinoxide; PNT, peptide nanotube nanocomposite; biotin-FNPs, biotinylated phenylalanine nanoparticles; Au, gold; rGO, reduced graphene oxide; RCA, rolling-circle amplification.

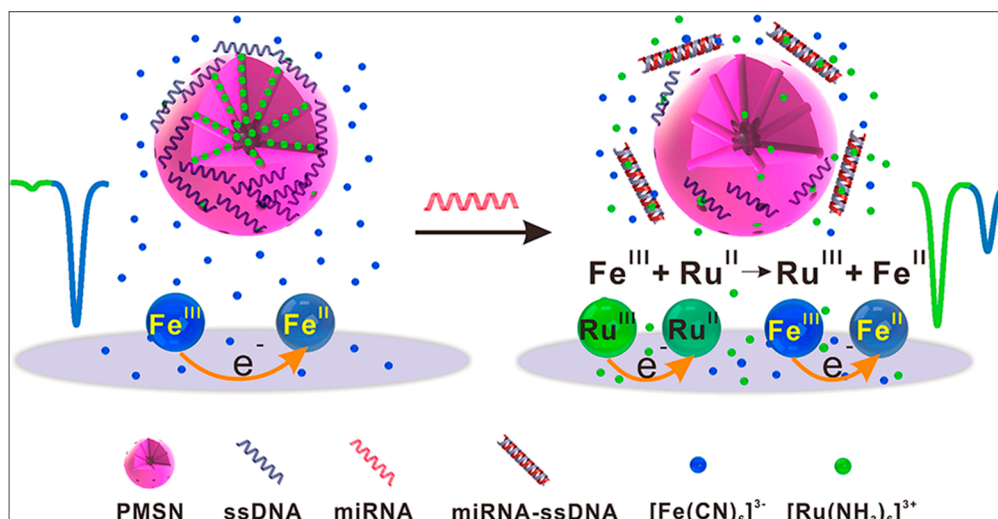


Figure 16. Scheme presenting the use of two free RedOx indicators reprinted from [180] with permission from (*Anal. Chem.* 2017, 89, 12293–11298). Copyright (2017) American Chemical Society.

6. Other Methods of MicroRNA Electrochemical Detection

Other methods were employed in the electrochemical biosensor area for the detection of miRNAs as biomarkers of cancer, including the guanine oxidation method, RedOx current of the electrode surface, and labeled miRNA.

6.1. Oxidation of Guanine

The guanine is a purine nucleobase present in miRNAs strands, which have RedOx active groups employed in the construction of the electrochemical biosensors. The approach of following the oxidation of guanine presents the first approach used in the case of a DNA biosensor and could be used also for miRNA detection. Akbarnia et al. [187] proposed enzymatic digestion biosensors for femtomolar detection of miRNA-541 as lung cancer biomarkers. Indeed, the probe is immobilized on the pencil graphite electrode modified graphene quantum dots (GQDs/PGE). Meanwhile, in the presence of miRNA-541, Hinf1 as a restriction enzyme cleaved the formed capture probe–miRNA-541 duplex. The oxidation of guanine was measured in the presence and absence of miRNA-541. After hybridization, a decrease in guanine's electrochemical signal was observed, because the DNA strands containing guanine were removed by the enzyme. In another use of the guanine oxidation method, Azab et al. [188] described a very sensitive biosensor at a zeptomolar level for miRNA let7-a detection using complementary sequence capture probe free-guanine bases. The capture probe was immobilized on the carbon paste electrode/carbon nanotubes/chrysin/gold nanoparticles (CPE/CNT/C/AuNPs) platform. The CNT/C film increases the surface area of the biosensor platform, increasing the conductivity, and thus is responsible for signal amplification.

The current method is very simple but has some limitations, especially considering that the oxidation of guanine bases as a free molecule is easier than in DNA strands and so could generate an unreliable result. As a matter of fact, the integration of a probe sequence without guanine, and its replacement with inosine that does not have the same potential for oxidation of guanine, is necessary in order to obtain only guanine oxidation response after the hybridization step (OFF-ON signal). Therefore, because the binding between cytosine and guanine is stronger than the binding of guanine with inosine, the use of such sequence does not provide a higher level of binding between the probe and miRNA compared to the sequence of the guanine-continuing DNA probe. Moreover, this method does not allow the regeneration of the biosensor because the oxidation of guanine is irreversible.

6.2. RedOx Current from Electrode Surface

Electrochemical biosensors designed for the detection of miRNAs based on RedOx current from the electrode surface were dismantled as a detection method. This method consists of modifying the electrode surface with an electroactive molecule before immobilizing the capture. The detection of miRNAs is done by electrochemical monitoring of the response of the redox molecule deposited on the electrode surface before and after the hybridization probe [189–191]. For this purpose, a simple model has recently been described by Zouari et al. [192] for the quantification of miRNA-21 at fM level, using screen-printed carbon electrode/pyrene carboxylic acid/rGO/AuNPs as biosensor platform. A 6-ferrocenylhexanethiol (Fc-SH) as a RedOx molecule was immobilized on the electrode surface.

6.3. Labeled MicroRNA

This method needs a labeled miRNA, which provides a hard step for the biosensor application in real samples. A labeled miRNA biosensor was recently described by Sabahi et al. [193] for the quantification of miRNA-21 at fM level. This was obtained by the use of cadmium ions (Cd^{2+}) which is linked to a phosphate group of miRNA via an electrostatic reaction. Then, the labeled miRNA hybridize with a capture probe immobilized on a fluorine-doped tin oxide electrode/SWCNTs/dendritic gold nanostructures through to Au–thiol interaction.

7. Conclusions and Future Perspectives

This work reviewed the progress in the development of electrochemical miRNAs biosensors using different approaches based on an electroactive species-labeled probe sequence, catalyst, RedOx intercalating agent, RedOx system, among others. In view of the various published papers, all miRNA strategies of detection based on electrochemical biosensors discussed in this review are presented according to their percentage of use (Figure 17). This distribution indicated clearly that the RedOx indicator as labeled, intercalant, or free RedOx indicator is widely used for miRNA detection with a percentage of 69% compared to catalytic detection, which presents 26%. In general, all approaches discussed in this review have almost equal use for miRNA detection, except the categories of other methods, which are still not developed yet compared to their employment in DNA biosensors. This is due probably to the lack of the association of these methods with the amplification approach generally used in the case of miRNA detection.

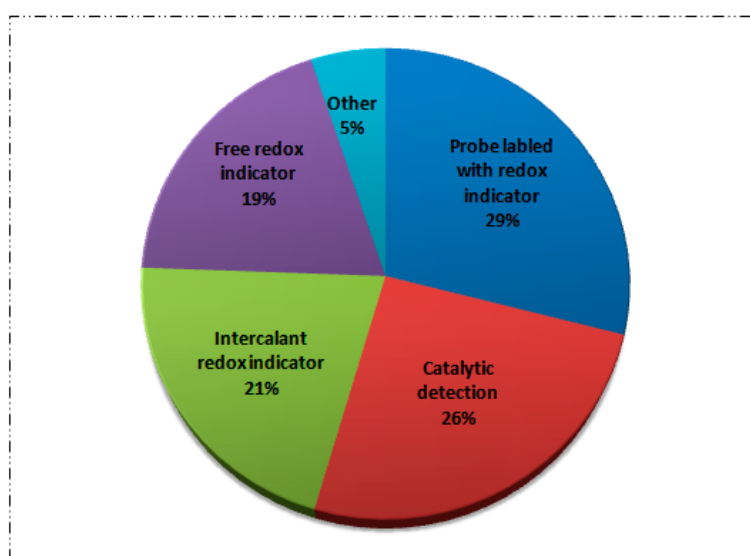


Figure 17. Distribution percentage of different microRNA strategies detection based on electrochemical biosensors.

The synthesis study clearly showed that electrochemical biosensors are efficient and practical approaches towards the analysis of miRNAs in the clinical field with high sensitivity. Nevertheless, the problem of miRNA analysis in the real sample cannot be neglected regarding the intercalating agent RedOx and the free RedOx indicator. These approaches have certain limitations, including the likely occurrence in the real sample of interferences, which could affect the results obtained. Otherwise, approaches based on electroactive species labeled with a probe sequence and a catalyst enable an accurate and precise analysis of miRNAs in a real sample. In addition, simultaneously detecting two miRNAs is more favorable with the RedOx-labeled probe sequence strategy, compared to the other strategies discussed. Although the LODs of the discussed biosensors are very low, most of the biosensors have not been tested and validated with a large number of samples from cancer patients and control groups. On the other hand, given the fact that, in general, known miRNAs are not specific to a single pathology, particular attention must also be paid to the development of electrochemical biosensors dedicated to the simultaneous quantification of a group of miRNAs to facilitate cancer diagnosis with improved reliability.

Although electrochemistry stands out due to its inherent miniaturization, mass production, and low cost, there are still significant challenges to meet before portable, robust, user-friendly point-of-care biosensors for cancer diagnosis through the detection of circulating miRNA expression profiles become a reality. Furthermore, because of these challenges, to date, to the best of our knowledge, no commercial electrochemical biosensor for circulating miRNA analysis is available; consequently, further effort should be devoted to validation, clinical assays, and the commercialization in the near future.

Author Contributions: The manuscript was written through contributions of all authors. All authors have read and agreed to the published version of the manuscript.

Funding: This research received no external funding.

Conflicts of Interest: The authors declare no conflict of interest.

References

1. Roointan, A.; Mir, T.A.; Wani, S.I.; Rehman, M.; Hussain, K.K.; Ahmed, B.; Abraham, S.; Savardashtaki, A.; Gandomani, G.; Gandomani, M.; et al. Early detection of lung cancer biomarkers through biosensor technology: A review. *J. Pharm. Biomed. Anal.* **2019**, *164*, 93–103. [[CrossRef](#)] [[PubMed](#)]
2. Schootman, M.; Fuortes, L.; Aft, R. Prognosis of metachronous contralateral breast cancer according to stage at diagnosis: The importance of early detection. *Breast Cancer Res. Treat.* **2006**, *99*, 91–95. [[CrossRef](#)] [[PubMed](#)]
3. Lytras, D.; Connor, S.; Bosonnet, L.; Jayan, R.; Evans, J.; Hughes, M.; Garvey, C.; Ghaneh, P.; Sutton, R.; Vinjamuri, S.; et al. Positron Emission Tomography Does Not Add to Computed Tomography for the Diagnosis and Staging of Pancreatic Cancer. *Dig. Surg.* **2005**, *22*, 55–62. [[CrossRef](#)] [[PubMed](#)]
4. Portalez, D.; Mozer, P.; Cornud, F.; Renard-Penna, R.; Misrai, V.; Thoulouzan, M.; Malavaud, B. Validation of the European Society of Urogenital Radiology Scoring System for Prostate Cancer Diagnosis on Multiparametric Magnetic Resonance Imaging in a Cohort of Repeat Biopsy Patients. *Eur. Urol.* **2012**, *62*, 986–996. [[CrossRef](#)] [[PubMed](#)]
5. Wagner, P.D.; Verma, M.; Srivastava, S. Challenges for Biomarkers in Cancer Detection. *Ann. N. Y. Acad. Sci.* **2004**, *1022*, 9–16. [[CrossRef](#)] [[PubMed](#)]
6. Islam, N.; Masud, M.K.; Haque, H.; Hossain, S.A.; Yamauchi, Y.; Nguyen, N.-T.; Shiddiky, M.J. RNA Biomarkers: Diagnostic and Prognostic Potentials and Recent Developments of Electrochemical Biosensors. *Small Methods* **2017**, *1*, 1700131. [[CrossRef](#)]
7. Mittal, S.; Kaur, H.; Gautam, N.; Mantha, A.K. Biosensors for breast cancer diagnosis: A review of bioreceptors, biotransducers and signal amplification strategies. *Biosens. Bioelectron.* **2017**, *88*, 217–231. [[CrossRef](#)]
8. Mousa, S.A. Biosensors: The new wave in cancer diagnosis. *Nanotechnol. Sci. Appl.* **2010**, *4*, 1–10. [[CrossRef](#)]

9. Hasanzadeh, M.; Shadjou, N.; De La Guardia, M. Early stage screening of breast cancer using electrochemical biomarker detection. *TrAC Trends Anal. Chem.* **2017**, *91*, 67–76. [[CrossRef](#)]
10. Diaconu, I.; Cristea, C.; Harceaga, V.; Marrazza, G.; Berindan-Neagoe, I.; Săndulescu, R. Electrochemical immunosensors in breast and ovarian cancer. *Clin. Chim. Acta* **2013**, *425*, 128–138. [[CrossRef](#)]
11. Yang, H.; Wang, J.; Yang, C.; Zhao, X.; Xie, S.; Ge, Z. Nano Pt@ZIF8 Modified Electrode and Its Application to Detect Sarcosine. *J. Electrochem. Soc.* **2018**, *165*, H247–H250. [[CrossRef](#)]
12. Filella, X.; Fernández-Galán, E.; Bonifacio, R.F.; Foj, L. Emerging biomarkers in the diagnosis of prostate cancer. *Pharm. Pers. Med.* **2018**, *11*, 83–94. [[CrossRef](#)] [[PubMed](#)]
13. Vaarala, M.H.; Porvari, K.; Lukkarinen, O.; Vihko, P. TheTMPRSS2 gene encoding transmembrane serine protease is overexpressed in a majority of prostate cancer patients: Detection of mutatedTMPRSS2 form in a case of aggressive disease. *Int. J. Cancer* **2001**, *94*, 705–710. [[CrossRef](#)]
14. Elshafey, R.; Tlili, C.; Abulrob, A.; Tavares, A.C.; Zourob, M. Label-free impedimetric immunosensor for ultrasensitive detection of cancer marker Murine double minute 2 in brain tissue. *Biosens. Bioelectron.* **2013**, *39*, 220–225. [[CrossRef](#)] [[PubMed](#)]
15. Laocharoensuk, R. Development of Electrochemical Immunosensors towards Point-of-care Cancer Diagnostics: Clinically Relevant Studies. *Electroanalysis* **2016**, *28*, 1716–1729. [[CrossRef](#)]
16. Hasan, S.; Jacob, R.; Manne, U.; Paluri, R. Advances in pancreatic cancer biomarkers. *Oncol. Rev.* **2019**, *13*, 410. [[CrossRef](#)]
17. Matsuoka, T.; Yashiro, M. Biomarkers of gastric cancer: Current topics and future perspective. *World J. Gastroenterol.* **2018**, *24*, 2818–2832. [[CrossRef](#)]
18. Ashizawa, T.; Okada, R.; Suzuki, Y.; Takagi, M.; Yamazaki, T.; Sumi, T.; Aoki, T.; Ohnuma, S.; Aoki, T. Clinical significance of interleukin-6 (IL-6) in the spread of gastric cancer: Role of IL-6 as a prognostic factor. *Gastric Cancer* **2005**, *8*, 124–131. [[CrossRef](#)]
19. Lou, J.; Zhang, L.; Lv, S.; Zhang, C.; Jiang, S. Biomarkers for Hepatocellular Carcinoma. *Biomark. Cancer* **2017**, *9*, 1–9. [[CrossRef](#)]
20. Farzin, L.; Shamsipur, M. Recent advances in design of electrochemical affinity biosensors for low level detection of cancer protein biomarkers using nanomaterial-assisted signal enhancement strategies. *J. Pharm. Biomed. Anal.* **2018**, *147*, 185–210. [[CrossRef](#)]
21. Li, J.; Sherman-Baust, A.C.; Tsai-Turton, M.; Bristow, R.E.; Roden, R.B.S.; Morin, P.J. Claudin-containing exosomes in the peripheral circulation of women with ovarian cancer. *BMC Cancer* **2009**, *9*, 244. [[CrossRef](#)] [[PubMed](#)]
22. Altintas, Z.; Tothill, I. Biomarkers and biosensors for the early diagnosis of lung cancer. *Sens. Actuators B Chem.* **2013**, *188*, 988–998. [[CrossRef](#)]
23. Arya, S.K.; Bhansali, S. Lung Cancer and Its Early Detection Using Biomarker-Based Biosensors. *Chem. Rev.* **2011**, *111*, 6783–6809. [[CrossRef](#)] [[PubMed](#)]
24. Xie, Y.; Todd, N.W.; Liu, Z.; Zhan, M.; Fang, H.; Peng, H.; Alattar, M.; Deepak, J.; Stass, S.A.; Jiang, F. Altered miRNA expression in sputum for diagnosis of non-small cell lung cancer. *Lung Cancer* **2010**, *67*, 170–176. [[CrossRef](#)] [[PubMed](#)]
25. Lim, E.H.; Zhang, S.-L.; Li, J.-L.; Yap, W.-S.; Howe, T.-C.; Tan, B.-P.; Lee, Y.-S.; Wong, D.; Khoo, K.-L.; Seto, K.-Y.; et al. Using whole genome amplification (WGA) of low-volume biopsies to assess the prognostic role of EGFR, KRAS, p53, and CMET mutations in advanced-stage non-small cell lung cancer (NSCLC). *J. Thorac. Oncol.* **2009**, *4*, 12–21. [[CrossRef](#)] [[PubMed](#)]
26. Staden, R.-I.S.-V.; Comnea-Stancu, I.R.; Surdu-Bob, C.C. Molecular Screening of Blood Samples for the Simultaneous Detection of CEA, HER-1, NSE, CYFRA 21-1 Using Stochastic Sensors. *J. Electrochem. Soc.* **2017**, *164*, B267–B273. [[CrossRef](#)]
27. Carr, O.; Raymundo-Pereira, P.A.; Shimizu, F.M.; Sorroche, B.P.; Melendez, M.E.; Pedro, R.D.O.; Miranda, P.B.; Carvalho, A.L.; Reis, R.M.; Arantes, L.M.; et al. Genosensor made with a self-assembled monolayer matrix to detect MGMT gene methylation in head and neck cancer cell lines. *Talanta* **2020**, *210*, 120609. [[CrossRef](#)]
28. Lee, R.C.; Feinbaum, R.L.; Ambros, V. The *C. elegans* heterochronic gene *lin-4* encodes small RNAs with antisense complementarity to *lin-14*. *Cell* **1993**, *75*, 843–854. [[CrossRef](#)]

29. Negrini, M.; Ferracin, M.; Sabbioni, S.; Croce, C.M. MicroRNAs in human cancer: From research to therapy. *J. Cell Sci.* **2007**, *120*, 1833–1840. [[CrossRef](#)]
30. Tang, X.; Tang, G.; Özcan, S. Role of microRNAs in diabetes. *Biochim. Biophys. Acta BBA Bioenergy* **2008**, *1779*, 697–701. [[CrossRef](#)]
31. Chen, Y.-X.; Huang, K.-J.; Niu, K.-X. Recent advances in signal amplification strategy based on oligonucleotide and nanomaterials for microRNA detection—A review. *Biosens. Bioelectron.* **2018**, *99*, 612–624. [[CrossRef](#)] [[PubMed](#)]
32. Keshavarz, M.; Behpour, M.; Rafiee-Pour, H.-A. Recent trends in electrochemical microRNA biosensors for early detection of cancer. *RSC Adv.* **2015**, *5*, 35651–35660. [[CrossRef](#)]
33. Aziz, N.B.; Mahmudunnabi, R.G.; Umer, M.; Sharma, S.; Rashid, A.; Alhamhoom, Y.; Shim, Y.-B.; Salomon, C.; Shiddiky, M.J. MicroRNAs in ovarian cancer and recent advances in the development of microRNA-based biosensors. *Analyst* **2020**, *145*, 2038–2057. [[CrossRef](#)] [[PubMed](#)]
34. Miodek, A.; Mejri-Omrani, N.; Khoder, R.; Korri-Youssoufi, H.; Mejri, N. Electrochemical functionalization of polypyrrole through amine oxidation of poly(amidoamine) dendrimers: Application to DNA biosensor. *Talanta* **2016**, *154*, 446–454. [[CrossRef](#)] [[PubMed](#)]
35. Wang, Y.; Hsine, Z.; Sauriat-Dorizon, H.; Mlika, R.; Korri-Youssoufi, H. Structural and electrochemical studies of functionalization of reduced graphene oxide with alkoxyphenylporphyrin mono- and tetra- carboxylic acid: Application to DNA sensors. *Electrochim. Acta* **2020**, *357*, 136852. [[CrossRef](#)]
36. Yazdanparast, S.; Benvidi, A.; Azimzadeh, M.; Tezerjani, M.D.; Ghaani, M.R. Experimental and theoretical study for miR-155 detection through resveratrol interaction with nucleic acids using magnetic core-shell nanoparticles. *Microchim. Acta* **2020**, *187*, 1–10. [[CrossRef](#)]
37. Masud, M.K.; Umer, M.; Hossain, S.A.; Yamauchi, Y.; Nguyen, N.-T.; Shiddiky, M.J. Nanoarchitecture Frameworks for Electrochemical miRNA Detection. *Trends Biochem. Sci.* **2019**, *44*, 433–452. [[CrossRef](#)]
38. Chen, C. Recent Advances in Nanomaterials-Based Electrochemical Biosensors for MicroRNAs Detection. *Int. J. Electrochem. Sci.* **2019**, *14*, 5174–5187. [[CrossRef](#)]
39. Mujica, M.L.; Gallay, P.A.; Perrachione, F.; Montemerlo, A.E.; Tamborelli, L.A.; Vaschetti, V.M.; Reartes, D.F.; Bollo, S.; Rodríguez, M.C.; Dalmaso, P.R.; et al. New trends in the development of electrochemical biosensors for the quantification of microRNAs. *J. Pharm. Biomed. Anal.* **2020**, *189*, 113478. [[CrossRef](#)]
40. Mohammadi, H.; Yammouri, G.; Amine, A. Current advances in electrochemical genosensors for detecting microRNA cancer markers. *Curr. Opin. Electrochem.* **2019**, *16*, 96–105. [[CrossRef](#)]
41. Daneshpour, M.; Omidfar, K.; Ghanbarian, H. A novel electrochemical nanobiosensor for the ultrasensitive and specific detection of femtomolar-level gastric cancer biomarker miRNA-106a. *Beilstein J. Nanotechnol.* **2016**, *7*, 2023–2036. [[CrossRef](#)]
42. Sun, E.; Wang, L.; Zhou, X.; Ma, C.; Sun, Y.; Lei, M.; Lu, B.; Han, R. Retracted Article: Graphene oxide/DNA-decorated electrode for the fabrication of microRNA biosensor. *RSC Adv.* **2015**, *5*, 69334–69338. [[CrossRef](#)]
43. Yang, B.; Zhang, S.; Fang, X.; Kong, J. Double signal amplification strategy for ultrasensitive electrochemical biosensor based on nuclease and quantum dot-DNA nanocomposites in the detection of breast cancer 1 gene mutation. *Biosens. Bioelectron.* **2019**, *142*, 111544. [[CrossRef](#)] [[PubMed](#)]
44. Rezaei, H.; Motovali-Bashi, M.; Radfar, S. An enzyme-free electrochemical biosensor for simultaneous detection of two hemophilia A biomarkers: Combining target recycling with quantum dots-encapsulated metal-organic frameworks for signal amplification. *Anal. Chim. Acta* **2019**, *1092*, 66–74. [[CrossRef](#)] [[PubMed](#)]
45. Tian, R.; Ning, W.; Chen, M.; Zhang, C.; Li, Q.; Bai, J. High performance electrochemical biosensor based on 3D nitrogen-doped reduced graphene oxide electrode and tetrahedral DNA nanostructure. *Talanta* **2019**, *194*, 273–281. [[CrossRef](#)]
46. Chen, Z.; Xie, Y.; Huang, W.; Qin, C.; Yu, A.; Lai, G. Exonuclease-assisted target recycling for ultrasensitive electrochemical detection of microRNA at vertically aligned carbon nanotubes. *Nanoscale* **2019**, *11*, 11262–11269. [[CrossRef](#)]
47. Yammouri, G.; Mohammadi, H.; Amine, A. A Highly Sensitive Electrochemical Biosensor Based on Carbon Black and Gold Nanoparticles Modified Pencil Graphite Electrode for microRNA-21 Detection. *Chem. Afr.* **2019**, *2*, 291–300. [[CrossRef](#)]

48. Jou, A.F.-J.; Chen, Y.-J.; Li, Y.; Chang, Y.-F.; Lee, J.-J.; Liao, A.T.; Ho, J.-A.A. Target-Triggered, Dual Amplification Strategy for Sensitive Electrochemical Detection of a Lymphoma-associated MicroRNA. *Electrochim. Acta* **2017**, *236*, 190–197. [[CrossRef](#)]
49. Miao, P.; Jiang, Y.; Zhang, T.; Huang, Y.; Tang, Y. Electrochemical sensing of attomolar miRNA combining cascade strand displacement polymerization and reductant-mediated amplification. *Chem. Commun.* **2018**, *54*, 7366–7369. [[CrossRef](#)]
50. Wang, T.; Viennois, E.; Merlin, D.; Wang, G. Microelectrode miRNA Sensors Enabled by Enzymeless Electrochemical Signal Amplification. *Anal. Chem.* **2015**, *87*, 8173–8180. [[CrossRef](#)]
51. Miao, P.; Wang, B.; Yu, Z.; Zhao, J.; Tang, Y. Ultrasensitive electrochemical detection of microRNA with star trigon structure and endonuclease mediated signal amplification. *Biosens. Bioelectron.* **2015**, *63*, 365–370. [[CrossRef](#)] [[PubMed](#)]
52. Ma, X.; Xu, H.; Qian, K.; Kandawa-Schulz, M.; Miao, W.; Wang, Y. Electrochemical detection of microRNAs based on AuNPs/CNNS nanocomposite with Duplex-specific nuclease assisted target recycling to improve the sensitivity. *Talanta* **2020**, *208*, 120441. [[CrossRef](#)] [[PubMed](#)]
53. Yang, D.; Cheng, W.; Chen, X.; Tang, Y.; Miao, P. Ultrasensitive electrochemical detection of miRNA based on DNA strand displacement polymerization and Ca²⁺-dependent DNAzyme cleavage. *Analyst* **2018**, *143*, 5352–5357. [[CrossRef](#)] [[PubMed](#)]
54. Wang, W.; Jayachandran, S.; Li, M.; Xu, S.; Luo, X. Hyaluronic acid functionalized nanostructured sensing interface for voltammetric determination of microRNA in biological media with ultra-high sensitivity and ultra-low fouling. *Microchim. Acta* **2018**, *185*, 156. [[CrossRef](#)] [[PubMed](#)]
55. Zhang, X.; Yang, Z.; Chang, Y.; Qing, M.; Yuan, R.; Chai, Y. Novel 2D-DNA-Nanoprobe-Mediated Enzyme-Free-Target-Recycling Amplification for the Ultrasensitive Electrochemical Detection of MicroRNA. *Anal. Chem.* **2018**, *90*, 9538–9544. [[CrossRef](#)]
56. Fu, C.; Liu, C.; Wang, S.; Luo, F.; Lin, Z.; Chen, G. A signal-on homogeneous electrochemical biosensor for sequence-specific microRNA based on duplex-specific nuclease-assisted target recycling amplification. *Anal. Methods* **2016**, *8*, 7034–7039. [[CrossRef](#)]
57. Miao, P.; Wang, B.; Chen, X.; Li, X.; Tang, Y. Tetrahedral DNA Nanostructure-Based MicroRNA Biosensor Coupled with Catalytic Recycling of the Analyte. *ACS Appl. Mater. Interfaces* **2015**, *7*, 6238–6243. [[CrossRef](#)]
58. Miao, P.; Wang, B.; Meng, F.; Yin, J.; Tang, Y. Ultrasensitive Detection of MicroRNA through Rolling Circle Amplification on a DNA Tetrahedron Decorated Electrode. *Bioconjugate Chem.* **2015**, *26*, 602–607. [[CrossRef](#)]
59. Liu, H.; Bei, X.; Xia, Q.; Fu, Y.; Zhang, S.; Liu, M.; Fan, K.; Zhang, M.; Yang, Y. Enzyme-free electrochemical detection of microRNA-21 using immobilized hairpin probes and a target-triggered hybridization chain reaction amplification strategy. *Microchim. Acta* **2015**, *183*, 297–304. [[CrossRef](#)]
60. Xu, S.; Chang, Y.; Wu, Z.; Li, Y.; Yuan, R.; Chai, Y.-Q. One DNA circle capture probe with multiple target recognition domains for simultaneous electrochemical detection of miRNA-21 and miRNA-155. *Biosens. Bioelectron.* **2020**, *149*, 111848. [[CrossRef](#)]
61. Yao, J.; Zhang, Z.; Deng, Z.; Wang, Y.; Guo, Y. An enzyme free electrochemical biosensor for sensitive detection of miRNA with a high discrimination factor by coupling the strand displacement reaction and catalytic hairpin assembly recycling. *Analyst* **2017**, *142*, 4116–4123. [[CrossRef](#)] [[PubMed](#)]
62. Zhou, L.; Wang, J.; Chen, Z.; Li, J.; Wang, T.; Zhang, Z.; Xie, G. A universal electrochemical biosensor for the highly sensitive determination of microRNAs based on isothermal target recycling amplification and a DNA signal transducer triggered reaction. *Microchim. Acta* **2017**, *184*, 1305–1313. [[CrossRef](#)]
63. Xiong, E.; Zhang, X.; Liu, Y.; Zhou, J.; Yu, P.; Li, X.; Chen, J. Ultrasensitive Electrochemical Detection of Nucleic Acids Based on the Dual-Signaling Electrochemical Ratiometric Method and Exonuclease III-Assisted Target Recycling Amplification Strategy. *Anal. Chem.* **2015**, *87*, 7291–7296. [[CrossRef](#)] [[PubMed](#)]
64. Zhang, J.; Wang, L.-L.; Hou, M.-F.; Xia, Y.-K.; He, W.-H.; Yan, A.; Weng, Y.-P.; Zeng, L.-P.; Chen, J. A ratiometric electrochemical biosensor for the exosomal microRNAs detection based on bipedal DNA walkers propelled by locked nucleic acid modified toehold mediate strand displacement reaction. *Biosens. Bioelectron.* **2018**, *102*, 33–40. [[CrossRef](#)]
65. Li, X.; Dou, B.; Yuan, R.; Xiang, Y. Mismatched catalytic hairpin assembly and ratiometric strategy for highly sensitive electrochemical detection of microRNA from tumor cells. *Sens. Actuators B Chem.* **2019**, *286*, 191–197. [[CrossRef](#)]

66. Cheng, F.-F.; He, T.-T.; Miao, H.-T.; Shi, J.-J.; Jiang, L.-P.; Zhu, J. Electron Transfer Mediated Electrochemical Biosensor for MicroRNAs Detection Based on Metal Ion Functionalized Titanium Phosphate Nanospheres at Attomole Level. *ACS Appl. Mater. Interfaces* **2015**, *7*, 2979–2985. [[CrossRef](#)]
67. Li, X.-M.; Wang, L.-L.; Luo, J.; Wei, Q.-L. A dual-amplified electrochemical detection of mRNA based on duplex-specific nuclease and bio-bar-code conjugates. *Biosens. Bioelectron.* **2015**, *65*, 245–250. [[CrossRef](#)]
68. Luo, L.; Wang, L.; Zeng, L.; Wang, Y.; Weng, Y.; Liao, Y.; Chen, T.; Xia, Y.; Zhang, J.; Chen, J. A ratiometric electrochemical DNA biosensor for detection of exosomal MicroRNA. *Talanta* **2020**, *207*, 120298. [[CrossRef](#)]
69. Tao, Y.; Yin, D.; Jin, M.; Fang, J.; Dai, T.; Li, Y.; Li, Y.; Pu, Q.; Xie, G. Double-loop hairpin probe and doxorubicin-loaded gold nanoparticles for the ultrasensitive electrochemical sensing of microRNA. *Biosens. Bioelectron.* **2017**, *96*, 99–105. [[CrossRef](#)]
70. Yuan, Y.-H.; Chi, B.-Z.; Wen, S.-H.; Liang, R.-P.; Li, Z.-M.; Qiu, J.-D. Ratiometric electrochemical assay for sensitive detecting microRNA based on dual-amplification mechanism of duplex-specific nuclease and hybridization chain reaction. *Biosens. Bioelectron.* **2018**, *102*, 211–216. [[CrossRef](#)]
71. Zouari, M.; Campuzano, S.; Pingarrón, J.; Raouafi, N. Femtomolar direct voltammetric determination of circulating miRNAs in sera of cancer patients using an enzymeless biosensor. *Anal. Chim. Acta* **2020**, *1104*, 188–198. [[CrossRef](#)] [[PubMed](#)]
72. Yuan, Y.-H.; Wu, Y.-D.; Chi, B.-Z.; Wen, S.-H.; Liang, R.-P.; Qiu, J.-D. Simultaneously electrochemical detection of microRNAs based on multifunctional magnetic nanoparticles probe coupling with hybridization chain reaction. *Biosens. Bioelectron.* **2017**, *97*, 325–331. [[CrossRef](#)] [[PubMed](#)]
73. Mohammadniaeia, M.; Goa, A.; Chavan, S.G.; Koyappayila, A.; Kimb, S.-E.; Yoo, H.J.; Min, J.; Lee, M.-H. Relay-race RNA/barcode gold nanoflower hybrid for wide and sensitive detection of microRNA in total patient serum. *Biosens. Bioelectron.* **2019**, *141*, 111468. [[CrossRef](#)] [[PubMed](#)]
74. Zhang, J.; Hun, X. Electrochemical determination of miRNA-155 using molybdenum carbide nanosheets and colloidal gold modified electrode coupled with mismatched catalytic hairpin assembly strategy. *Microchem. J.* **2019**, *150*, 104095. [[CrossRef](#)]
75. Tian, L.; Qi, J.; Ma, X.; Wang, X.; Yao, C.; Song, W.; Wang, Y. A facile DNA strand displacement reaction sensing strategy of electrochemical biosensor based on N-carboxymethyl chitosan/molybdenum carbide nanocomposite for microRNA-21 detection. *Biosens. Bioelectron.* **2018**, *122*, 43–50. [[CrossRef](#)]
76. Miao, P.; Tang, Y.; Zhang, Q.; Bo, B.; Wang, J. Identification of Cellular MicroRNA Coupling Strand Displacement Polymerization and Nicking-Endonuclease-Based Cleavage. *ChemPlusChem* **2015**, *80*, 1712–1715. [[CrossRef](#)]
77. Miao, P.; Tang, Y.; Yin, J. MicroRNA detection based on analyte triggered nanoparticle localization on a tetrahedral DNA modified electrode followed by hybridization chain reaction dual amplification. *Chem. Commun.* **2015**, *51*, 15629–15632. [[CrossRef](#)]
78. Que, H.; Zhang, D.; Guoa, B.; Wang, T.; Wua, H.; Hana, D.; Yan, Y. Label-free and ultrasensitive electrochemical biosensor for the detection of EBV-related DNA based on AgDNCs@DNA/AgNCs nanocomposites and lambda exonuclease-assisted target recycling. *Biosens. Bioelectron.* **2019**, *143*, 111610. [[CrossRef](#)]
79. Cheng, W.; Ma, J.; Cao, P.; Zhang, Y.; Xu, C.; Yi, Y.; Li, J. Enzyme-free electrochemical biosensor based on double signal amplification strategy for the ultra-sensitive detection of exosomal microRNAs in biological samples. *Talanta* **2020**, *219*, 121242. [[CrossRef](#)]
80. Hakimian, F.; Ghourchian, H. Ultrasensitive electrochemical biosensor for detection of microRNA-155 as a breast cancer risk factor. *Anal. Chim. Acta* **2020**, *1136*, 1–8. [[CrossRef](#)]
81. Deng, K.; Liu, X.; Li, C.; Huang, H. Sensitive electrochemical sensing platform for microRNAs detection based on shortened multi-walled carbon nanotubes with high-loaded thionin. *Biosens. Bioelectron.* **2018**, *117*, 168–174. [[CrossRef](#)] [[PubMed](#)]
82. Yu, N.; Wang, Z.; Wang, C.; Han, J.; Bu, H. Combining padlock exponential rolling circle amplification with CoFe₂O₄ magnetic nanoparticles for microRNA detection by nanoelectrocatalysis without a substrate. *Anal. Chim. Acta* **2017**, *962*, 24–31. [[CrossRef](#)] [[PubMed](#)]
83. Meng, T.; Jia, H.; An, S.; Wang, H.; Yang, X.; Zhang, Y. Pd nanoparticles-DNA layered nanoreticulation biosensor based on target-catalytic hairpin assembly for ultrasensitive and selective biosensing of microRNA-21. *Sens. Actuators B Chem.* **2020**, *323*, 128621. [[CrossRef](#)]

84. Tang, H.; Zhu, J.; Wang, D.; Li, Y. Dual-signal amplification strategy for miRNA sensing with high sensitivity and selectivity by use of single Au nanowire electrodes. *Biosens. Bioelectron.* **2019**, *131*, 88–94. [[CrossRef](#)] [[PubMed](#)]
85. Ge, L.; Wang, W.; Li, F. Electro-Grafted Electrode with Graphene-Oxide-Like DNA Affinity for Ratiometric Homogeneous Electrochemical Biosensing of MicroRNA. *Anal. Chem.* **2017**, *89*, 11560–11567. [[CrossRef](#)]
86. Li, B.; Liu, F.; Peng, Y.; Yin, H.; Fan, W.; Yin, H.; Ai, S.; Zhang, X.-S. Two-stage cyclic enzymatic amplification method for ultrasensitive electrochemical assay of microRNA-21 in the blood serum of gastric cancer patients. *Biosens. Bioelectron.* **2016**, *79*, 307–312. [[CrossRef](#)]
87. Shen, Z.; He, L.; Wang, W.; Tan, L.; Gan, N. Highly sensitive and simultaneous detection of microRNAs in serum using stir-bar assisted magnetic DNA nanospheres-encoded probes. *Biosens. Bioelectron.* **2019**, *148*, 111831. [[CrossRef](#)]
88. Fu, P.; Xing, S.; Xu, M.; Zhao, Y.; Zhao, C. Peptide nucleic acid-based electrochemical biosensor for simultaneous detection of multiple microRNAs from cancer cells with catalytic hairpin assembly amplification. *Sens. Actuators B Chem.* **2020**, *305*, 127545. [[CrossRef](#)]
89. Azzouzi, S.; Fredj, Z.; Turner, A.P.F.; Ben Ali, M.; Mak, W.C. Generic Neutravidin Biosensor for Simultaneous Multiplex Detection of MicroRNAs via Electrochemically Encoded Responsive Nanolabels. *ACS Sens.* **2019**, *4*, 326–334. [[CrossRef](#)]
90. Mohammadniaei, M.; Koyappayil, A.; Sun, Y.; Min, J.; Lee, M.-H. Gold nanoparticle/MXene for multiple and sensitive detection of oncomiRs based on synergetic signal amplification. *Biosens. Bioelectron.* **2020**, *159*, 112208. [[CrossRef](#)]
91. Kuah, E.; Toh, S.; Yee, J.; Ma, Q.; Gao, Z. Enzyme Mimics: Advances and Applications. *Chem. A Eur. J.* **2016**, *22*, 8404–8430. [[CrossRef](#)] [[PubMed](#)]
92. Kosman, J.; Juskowiak, B. Peroxidase-mimicking DNAzymes for biosensing applications: A review. *Anal. Chim. Acta* **2011**, *707*, 7–17. [[CrossRef](#)] [[PubMed](#)]
93. Wang, M.; Shen, B.; Yuan, R.; Cheng, W.; Xu, H.; Ding, S. An electrochemical biosensor for highly sensitive determination of microRNA based on enzymatic and molecular beacon mediated strand displacement amplification. *J. Electroanal. Chem.* **2015**, *756*, 147–152. [[CrossRef](#)]
94. Ma, W.; Situ, B.; Lv, W.; Li, B.; Yin, X.; Vadgama, P.; Zheng, L.; Wang, W. Electrochemical determination of microRNAs based on isothermal strand-displacement polymerase reaction coupled with multienzyme functionalized magnetic micro-carriers. *Biosens. Bioelectron.* **2016**, *80*, 344–351. [[CrossRef](#)] [[PubMed](#)]
95. Yang, J.; Tang, M.; Diao, W.; Cheng, W.; Zhang, Y.; Yan, Y. Electrochemical strategy for ultrasensitive detection of microRNA based on MNase-mediated rolling circle amplification on a gold electrode. *Microchim. Acta* **2016**, *183*, 3061–3067. [[CrossRef](#)]
96. Wang, H.; Zuo, Z.; Ren, L.; Yuan, R.; Li, Q.; Ding, S.; Luo, R. Ultrasensitive electrochemical biosensing strategy for microRNA-21 detection based on homogeneous target-initiated transcription amplification. *J. Electroanal. Chem.* **2016**, *783*, 22–27. [[CrossRef](#)]
97. Xia, N.; Zhang, Y.; Wei, X.; Huang, Y.; Liu, L. An electrochemical microRNAs biosensor with the signal amplification of alkaline phosphatase and electrochemical–chemical–chemical redox cycling. *Anal. Chim. Acta* **2015**, *878*, 95–101. [[CrossRef](#)]
98. Shuai, H.-L.; Huang, K.-J.; Zhang, W.-J.; Cao, X.; Jia, M.-P. Sandwich-type microRNA biosensor based on magnesium oxide nanoflower and graphene oxide–gold nanoparticles hybrids coupling with enzyme signal amplification. *Sens. Actuators B Chem.* **2017**, *243*, 403–411. [[CrossRef](#)]
99. Mandli, J.; Mohammadi, H.; Amine, A. Electrochemical DNA sandwich biosensor based on enzyme amplified microRNA-21 detection and gold nanoparticles. *Bioelectrochemistry* **2017**, *116*, 17–23. [[CrossRef](#)]
100. Zouari, M.; Campuzano, S.; Pingarrón, J.M.; Raouafi, N.; Campuzano, S. Competitive RNA-RNA hybridization-based integrated nanostructured-disposable electrode for highly sensitive determination of miRNAs in cancer cells. *Biosens. Bioelectron.* **2017**, *91*, 40–45. [[CrossRef](#)]
101. Chen, Y.-X.; Zhang, W.-J.; Huang, K.-J.; Zheng, M.; Mao, Y.-C. An electrochemical microRNA sensing platform based on tungsten diselenide nanosheets and competitive RNA–RNA hybridization. *Analyst* **2017**, *142*, 4843–4851. [[CrossRef](#)] [[PubMed](#)]

102. Torrente-Rodríguez, R.M.; Montiel, V.R.-V.; Campuzano, S.; Farchado-Dinia, M.; Barderas, R.; Segundo-Acosta, P.S.; Montoya, J.J.; Pingarrón, J.M. Fast Electrochemical miRNAs Determination in Cancer Cells and Tumor Tissues with Antibody-Functionalized Magnetic Microcarriers. *ACS Sens.* **2016**, *1*, 896–903. [[CrossRef](#)]
103. Zeng, D.; Wang, Z.; Meng, Z.; Wang, P.; San, L.; Wang, W.; Aldalbahi, A.; Lili, S.; Shen, J.; Mi, X. DNA Tetrahedral Nanostructure-Based Electrochemical miRNA Biosensor for Simultaneous Detection of Multiple miRNAs in Pancreatic Carcinoma. *ACS Appl. Mater. Interfaces* **2017**, *9*, 24118–24125. [[CrossRef](#)] [[PubMed](#)]
104. Zhai, Q.; He, Y.; Li, X.; Guo, J.; Li, S.; Yi, G. A simple and ultrasensitive electrochemical biosensor for detection of microRNA based on hybridization chain reaction amplification. *J. Electroanal. Chem.* **2015**, *758*, 20–25. [[CrossRef](#)]
105. Torrente-Rodríguez, R.; Campuzano, S.; Montiel, V.R.-V.; Montoya, J.J.; Pingarrón, J.M.; Campuzano, S. Sensitive electrochemical determination of miRNAs based on a sandwich assay onto magnetic microcarriers and hybridization chain reaction amplification. *Biosens. Bioelectron.* **2016**, *86*, 516–521. [[CrossRef](#)] [[PubMed](#)]
106. Liu, L.; Gao, Y.; Liu, H.; Xia, N. An ultrasensitive electrochemical miRNAs sensor based on miRNAs-initiated cleavage of DNA by duplex-specific nuclease and signal amplification of enzyme plus redox cycling reaction. *Sens. Actuators B Chem.* **2015**, *208*, 137–142. [[CrossRef](#)]
107. Shuai, H.-L.; Huang, K.-J.; Chen, Y.-X.; Fang, L.-X.; Jia, M.-P. Au nanoparticles/hollow molybdenum disulfide microcubes based biosensor for microRNA-21 detection coupled with duplex-specific nuclease and enzyme signal amplification. *Biosens. Bioelectron.* **2017**, *89*, 989–997. [[CrossRef](#)]
108. Wang, J.; Lu, J.; Dong, S.; Zhu, N.; Gyimah, E.; Wang, K.; Li, Y.; Zhang, Z. An ultrasensitive electrochemical biosensor for detection of microRNA-21 based on redox reaction of ascorbic acid/iodine and duplex-specific nuclease assisted target recycling. *Biosens. Bioelectron.* **2019**, *130*, 81–87. [[CrossRef](#)]
109. Chen, Y.-X.; Wu, X.; Huang, K.-J. A sandwich-type electrochemical biosensing platform for microRNA-21 detection using carbon sphere-MoS₂ and catalyzed hairpin assembly for signal amplification. *Sens. Actuators B Chem.* **2018**, *270*, 179–186. [[CrossRef](#)]
110. Zhang, Y.; Yan, Y.; Chen, W.; Cheng, W.; Li, S.; Ding, X.; Li, D.; Wang, H.; Ju, H.; Ding, S. A simple electrochemical biosensor for highly sensitive and specific detection of microRNA based on mismatched catalytic hairpin assembly. *Biosens. Bioelectron.* **2015**, *68*, 343–349. [[CrossRef](#)]
111. Shuai, H.-L.; Huang, K.-J.; Xing, L.-L.; Chen, Y.-X. Ultrasensitive electrochemical sensing platform for microRNA based on tungsten oxide-graphene composites coupling with catalyzed hairpin assembly target recycling and enzyme signal amplification. *Biosens. Bioelectron.* **2016**, *86*, 337–345. [[CrossRef](#)] [[PubMed](#)]
112. Li, Q.; Zeng, F.; Lyu, N.; Liang, J. Highly sensitive and specific electrochemical biosensor for microRNA-21 detection by coupling catalytic hairpin assembly with rolling circle amplification. *Analyst* **2018**, *143*, 2304–2309. [[CrossRef](#)] [[PubMed](#)]
113. Zhang, H.; Fan, M.; Jiang, J.; Shen, Q.; Cai, C.; Shen, J. Sensitive electrochemical biosensor for MicroRNAs based on duplex-specific nuclease-assisted target recycling followed with gold nanoparticles and enzymatic signal amplification. *Anal. Chim. Acta* **2019**, *1064*, 33–39. [[CrossRef](#)] [[PubMed](#)]
114. Fang, C.S.; Kim, K.-S.; Yu, B.; Jon, S.; Kim, M.-S.; Yang, H. Ultrasensitive Electrochemical Detection of miRNA-21 Using a Zinc Finger Protein Specific to DNA–RNA Hybrids. *Anal. Chem.* **2017**, *89*, 2024–2031. [[CrossRef](#)]
115. Zouari, M.; Campuzano, S.; Pingarrón, J.M.; Raouafi, N. Amperometric Biosensing of miRNA-21 in Serum and Cancer Cells at Nanostructured Platforms Using Anti-DNA-RNA Hybrid Antibodies. *ACS Omega* **2018**, *3*, 8923–8931. [[CrossRef](#)]
116. Vargas, E.; Torrente-Rodríguez, R.; Montiel, V.R.-V.; Povedano, E.; Pedrero, M.; Montoya, J.J.; Campuzano, S.; Pingarrón, J.M. Magnetic Beads-Based Sensor with Tailored Sensitivity for Rapid and Single-Step Amperometric Determination of miRNAs. *Int. J. Mol. Sci.* **2017**, *18*, 2151. [[CrossRef](#)]
117. Zouari, M.; Campuzano, S.; Pingarrón, J.; Raouafi, N. Ultrasensitive determination of microribonucleic acids in cancer cells with nanostructured-disposable electrodes using the viral protein p19 for recognition of ribonucleic acid/microribonucleic acid homoduplexes. *Electrochim. Acta* **2018**, *262*, 39–47. [[CrossRef](#)]
118. Hu, T.; Zhang, L.; Wen, W.; Zhang, X.; Wang, S. Enzyme catalytic amplification of miRNA-155 detection with graphene quantum dot-based electrochemical biosensor. *Biosens. Bioelectron.* **2016**, *77*, 451–456. [[CrossRef](#)]

119. Zhang, H.; Wang, Q.; Yang, X.; Wang, K.; Li, Q.; Li, Z.; Gao, L.; Nie, W.; Zheng, Y. An isothermal electrochemical biosensor for the sensitive detection of microRNA based on a catalytic hairpin assembly and supersandwich amplification. *Analyst* **2017**, *142*, 389–396. [[CrossRef](#)]
120. Wang, H.; Jian, Y.; Kong, Q.; Liu, H.; Lan, F.; Liang, L.; Ge, S.; Yu, J. Ultrasensitive electrochemical paper-based biosensor for microRNA via strand displacement reaction and metal-organic frameworks. *Sens. Actuators B Chem.* **2018**, *257*, 561–569. [[CrossRef](#)]
121. Wang, Z.; Si, L.; Bao, J.; Dai, Z. A reusable microRNA sensor based on the electrocatalytic property of heteroduplex-templated copper nanoclusters. *Chem. Commun.* **2015**, *51*, 6305–6307. [[CrossRef](#)] [[PubMed](#)]
122. Zhang, K.; Dong, H.; Dai, W.; Meng, X.; Lu, H.; Wu, T.; Zhang, X. Fabricating Pt/Sn-In₂O₃ Nanoflower with Advanced Oxygen Reduction Reaction Performance for High-Sensitivity MicroRNA Electrochemical Detection. *Anal. Chem.* **2016**, *89*, 648–655. [[CrossRef](#)] [[PubMed](#)]
123. Guo, W.-J.; Wu, Z.; Yang, X.-Y.; Pang, D.-W.; Zhang, Z.-L. Ultrasensitive electrochemical detection of microRNA-21 with wide linear dynamic range based on dual signal amplification. *Biosens. Bioelectron.* **2019**, *131*, 267–273. [[CrossRef](#)] [[PubMed](#)]
124. Sun, X.; Wang, H.; Jian, Y.; Lan, F.; Zhang, L.; Liu, H.; Ge, S.; Yu, J. Ultrasensitive microfluidic paper-based electrochemical/visual biosensor based on spherical-like cerium dioxide catalyst for miR-21 detection. *Biosens. Bioelectron.* **2018**, *105*, 218–225. [[CrossRef](#)] [[PubMed](#)]
125. Lianga, Z.; Oua, D.; Sunab, D.; Tongc, Y.; Luo, H.-B.; Chen, Z. Ultrasensitive biosensor for microRNA-155 using synergistically catalytic nanoprobe coupled with improved cascade strand displacement reaction. *Biosens. Bioelectron.* **2019**, *146*, 111744. [[CrossRef](#)] [[PubMed](#)]
126. Wu, Y.; Sheng, K.; Liu, Y.; Yu, Q.; Ye, B. Enzyme spheres as novel tracing tags coupled with target-induced DNAzyme assembly for ultrasensitive electrochemical microRNA assay. *Anal. Chim. Acta* **2016**, *948*, 1–8. [[CrossRef](#)]
127. Zhou, L.; Wang, T.; Bai, Y.; Li, Y.; Qiu, J.; Yu, W.; Zhang, S. Dual-amplified strategy for ultrasensitive electrochemical biosensor based on click chemistry-mediated enzyme-assisted target recycling and functionalized fullerene nanoparticles in the detection of microRNA-141. *Biosens. Bioelectron.* **2020**, *150*, 111964. [[CrossRef](#)]
128. Lu, J.; Wang, J.; Hu, X.; Gyimah, E.; Yakubu, S.; Wang, K.; Wu, X.; Zhanga, Z. Electrochemical Biosensor Based on Tetrahedral DNA Nanostructures and G-Quadruplex–Hemin Conformation for the Ultrasensitive Detection of MicroRNA-21 in Serum. *Anal. Chem.* **2019**, *91*, 7353–7359. [[CrossRef](#)]
129. Liu, L.; Song, C.; Zhang, Z.; Yang, J.; Zhou, L.; Zhang, X.; Xie, G. Ultrasensitive electrochemical detection of microRNA-21 combining layered nanostructure of oxidized single-walled carbon nanotubes and nanodiamonds by hybridization chain reaction. *Biosens. Bioelectron.* **2015**, *70*, 351–357. [[CrossRef](#)]
130. Huang, Y.L.; Mo, S.; Gao, Z.F.; Chen, J.R.; Lei, J.L.; Luo, H.Q.; Li, N.B. Amperometric biosensor for microRNA based on the use of tetrahedral DNA nanostructure probes and guanine nanowire amplification. *Microchim. Acta* **2017**, *184*, 2597–2604. [[CrossRef](#)]
131. Cai, W.; Xie, S.; Tang, Y.; Chai, Y.; Yuan, R.; Zhang, J. A label-free electrochemical biosensor for microRNA detection based on catalytic hairpin assembly and in situ formation of molybdophosphate. *Talanta* **2017**, *163*, 65–71. [[CrossRef](#)] [[PubMed](#)]
132. Mohammadi, H.; Amine, A. Spectrophotometric and Electrochemical Determination of MicroRNA-155 Using Sandwich Hybridization Magnetic Beads. *Anal. Lett.* **2018**, *51*, 411–423. [[CrossRef](#)]
133. Jirakova, L.; Hrstka, R.; Campuzano, S.; Pingarrón, J.M.; Bartosik, M. Multiplexed Immunosensing Platform Coupled to Hybridization Chain Reaction for Electrochemical Determination of MicroRNAs in Clinical Samples. *Electroanalysis* **2018**, *31*, 293–302. [[CrossRef](#)]
134. Povedano, E.; Montiel, V.R.-V.; Gamella, M.; Serafín, V.; Pedrero, M.; Moranova, L.; Bartosik, M.; Montoya, J.J.; Yáñez-Sedeño, P.; Campuzano, S.; et al. A novel zinc finger protein-based amperometric biosensor for miRNA determination. *Anal. Bioanal. Chem.* **2020**, *412*, 5031–5041. [[CrossRef](#)]
135. Tian, L.; Qi, J.; Oderinde, O.; Yao, C.; Song, W.; Wang, Y. Planar intercalated copper (II) complex molecule as small molecule enzyme mimic combined with Fe₃O₄ nanozyme for bienzyme synergistic catalysis applied to the microRNA biosensor. *Biosens. Bioelectron.* **2018**, *110*, 110–117. [[CrossRef](#)]
136. Wang, J.; Hui, N.; Hui, N. Electrochemical functionalization of polypyrrole nanowires for the development of ultrasensitive biosensors for detecting microRNA. *Sens. Actuators B Chem.* **2019**, *281*, 478–485. [[CrossRef](#)]

137. Azimzadeh, M.; Rahaie, M.; Nasirizadeh, N.; Naderi-Manesh, H. Application of Oracet Blue in a novel and sensitive electrochemical biosensor for the detection of microRNA. *Anal. Methods* **2015**, *7*, 9495–9503. [[CrossRef](#)]
138. Tian, L.; Qian, K.; Qi, J.; Liu, Q.; Yao, C.; Song, W.; Wang, Y. Gold nanoparticles superlattices assembly for electrochemical biosensor detection of microRNA-21. *Biosens. Bioelectron.* **2018**, *99*, 564–570. [[CrossRef](#)]
139. Moccia, M.; Caratelli, V.; Cinti, S.; Pede, B.; Avitabile, C.; Saviano, M.; Imbriani, A.L.; Moscone, D.; Arduini, F. Paper-based electrochemical peptide nucleic acid (PNA) biosensor for detection of miRNA-492: A pancreatic ductal adenocarcinoma biomarker. *Biosens. Bioelectron.* **2020**, *165*, 112371. [[CrossRef](#)]
140. Zhang, C.; Li, D.; Li, D.; Wen, K.; Yang, X.; Zhu, Y. Rolling circle amplification-mediated in situ synthesis of palladium nanoparticles for the ultrasensitive electrochemical detection of microRNA. *Analyst* **2019**, *144*, 3817–3825. [[CrossRef](#)]
141. Ren, R.; Bi, Q.; Yuan, R.; Xiang, Y. An efficient, label-free and sensitive electrochemical microRNA sensor based on target-initiated catalytic hairpin assembly of trivalent DNAzyme junctions. *Sens. Actuators B Chem.* **2020**, *304*, 127068. [[CrossRef](#)]
142. Yang, C.; Shi, K.; Dou, B.; Xiang, Y.; Chai, Y.; Yuan, R. In Situ DNA-Templated Synthesis of Silver Nanoclusters for Ultrasensitive and Label-Free Electrochemical Detection of MicroRNA. *ACS Appl. Mater. Interfaces* **2015**, *7*, 1188–1193. [[CrossRef](#)] [[PubMed](#)]
143. Li, F.; Peng, J.; Zheng, Q.; Guo, X.; Tang, H.; Yao, S. Carbon Nanotube-Polyamidoamine Dendrimer Hybrid-Modified Electrodes for Highly Sensitive Electrochemical Detection of MicroRNA24. *Anal. Chem.* **2015**, *87*, 4806–4813. [[CrossRef](#)] [[PubMed](#)]
144. Bao, J.; Hou, C.; Zhao, Y.; Geng, X.; Samalo, M.; Yang, H.; Bian, M.; Huo, D. An enzyme-free sensitive electrochemical microRNA-16 biosensor by applying a multiple signal amplification strategy based on Au/PPy-rGO nanocomposite as a substrate. *Talanta* **2019**, *196*, 329–336. [[CrossRef](#)] [[PubMed](#)]
145. Zhang, W.; Xu, H.; Zhao, X.; Tang, X.; Yang, S.; Yu, L.; Zhao, S.; Chang, K.; Chen, M. 3D DNA nanonet structure coupled with target-catalyzed hairpin assembly for dual-signal synergistically amplified electrochemical sensing of circulating microRNA. *Anal. Chim. Acta* **2020**, *1122*, 39–47. [[CrossRef](#)] [[PubMed](#)]
146. Liu, S.; Yang, Z.; Chang, Y.; Chai, Y.; Yuan, R. An enzyme-free electrochemical biosensor combining target recycling with Fe₃O₄/CeO₂@Au nanocatalysts for microRNA-21 detection. *Biosens. Bioelectron.* **2018**, *119*, 170–175. [[CrossRef](#)]
147. Huang, S.; Li, J.; Jin, X.; Liu, Y.; Huang, S. Ultrasensitive electrochemical microRNA-21 biosensor coupling with carboxylate-reduced graphene oxide-based signal-enhancing and duplex-specific nuclease-assisted target recycling. *Sens. Actuators B Chem.* **2019**, *297*, 126740. [[CrossRef](#)]
148. Guo, J.; Yuan, C.; Yan, Q.; Duan, Q.; Li, X.; Yi, G. An electrochemical biosensor for microRNA-196a detection based on cyclic enzymatic signal amplification and template-free DNA extension reaction with the adsorption of methylene blue. *Biosens. Bioelectron.* **2018**, *105*, 103–108. [[CrossRef](#)]
149. Su, S.; Wu, Y.; Zhu, D.; Chao, J.; Liu, X.; Wan, Y.; Su, Y.; Zuo, X.; Fan, C.; Wang, L. On-Electrode Synthesis of Shape-Controlled Hierarchical Flower-Like Gold Nanostructures for Efficient Interfacial DNA Assembly and Sensitive Electrochemical Sensing of MicroRNA. *Small* **2016**, *12*, 3794–3801. [[CrossRef](#)]
150. Yu, S.; Wang, Y.; Jiang, L.-P.; Bi, S.; Zhu, J. Cascade Amplification-Mediated In Situ Hot-Spot Assembly for MicroRNA Detection and Molecular Logic Gate Operations. *Anal. Chem.* **2018**, *90*, 4544–4551. [[CrossRef](#)]
151. Chen, X.; Yao, L.; Wang, Y.-C.; Chen, Q.; Deng, H.; Lin, Z.; Yang, H.-H. Novel electrochemical nanoswitch biosensor based on self-assembled pH-sensitive continuous circular DNA. *Biosens. Bioelectron.* **2019**, *131*, 274–279. [[CrossRef](#)] [[PubMed](#)]
152. Wang, S.; Lu, S.; Zhao, J.; Ye, J.; Huang, J.; Yang, X. An electric potential modulated cascade of catalyzed hairpin assembly and rolling chain amplification for microRNA detection. *Biosens. Bioelectron.* **2019**, *126*, 565–571. [[CrossRef](#)] [[PubMed](#)]
153. Wang, Y.-H.; Huang, K.-J.; Wu, X.; Ma, Y.-Y.; Song, D.-L.; Du, C.-Y.; Chang, S.-H. Ultrasensitive supersandwich-type biosensor for enzyme-free amplified microRNA detection based on N-doped graphene/Au nanoparticles and hemin/G-quadruplexes. *J. Mater. Chem. B* **2018**, *6*, 2134–2142. [[CrossRef](#)]
154. Asadzadeh-Firouzabadi, A.; Zare, H.R. Preparation and application of AgNPs/SWCNTs nanohybrid as an electroactive label for sensitive detection of miRNA related to lung cancer. *Sens. Actuators B Chem.* **2018**, *260*, 824–831. [[CrossRef](#)]

155. Wang, F.; Chu, Y.; Ai, Y.; Chen, L.; Gao, F. Graphene oxide with in-situ grown Prussian Blue as an electrochemical probe for microRNA-122. *Microchim. Acta* **2019**, *186*, 116. [[CrossRef](#)]
156. Liu, L.; Chang, Y.; Xia, N.; Peng, P.; Zhang, L.; Jiang, M.; Zhang, J.; Liu, L. Simple, sensitive and label-free electrochemical detection of microRNAs based on the in situ formation of silver nanoparticles aggregates for signal amplification. *Biosens. Bioelectron.* **2017**, *94*, 235–242. [[CrossRef](#)]
157. Azimzadeh, M.; Rahaie, M.; Nasirizadeh, N.; Ashtari, K.; Naderi-Manesh, H. An electrochemical nanobiosensor for plasma miRNA-155, based on graphene oxide and gold nanorod, for early detection of breast cancer. *Biosens. Bioelectron.* **2016**, *77*, 99–106. [[CrossRef](#)]
158. Cui, L.; Wang, M.; Sun, B.; Ai, S.; Wang, S.; Zhang, C.-Y. Substrate-free and label-free electrocatalysis-assisted biosensor for sensitive detection of microRNA in lung cancer cells. *Chem. Commun.* **2019**, *55*, 1172–1175. [[CrossRef](#)]
159. Bo, B.; Zhang, T.; Jiang, Y.; Cui, H.; Miao, P. Triple Signal Amplification Strategy for Ultrasensitive Determination of miRNA Based on Duplex Specific Nuclease and Bridge DNA–Gold Nanoparticles. *Anal. Chem.* **2018**, *90*, 2395–2400. [[CrossRef](#)]
160. Su, S.; Cao, W.; Liu, W.; Lu, Z.; Zhu, D.; Chao, J.; Weng, L.; Wang, L.; Fan, C.; Wang, L. Dual-mode electrochemical analysis of microRNA-21 using gold nanoparticle-decorated MoS₂ nanosheet. *Biosens. Bioelectron.* **2017**, *94*, 552–559. [[CrossRef](#)]
161. Feng, K.; Liu, J.; Deng, L.; Yu, H.; Yang, M. Amperometric detection of microRNA based on DNA-controlled current of a molybdophosphate redox probe and amplification via hybridization chain reaction. *Microchim. Acta* **2017**, *185*, 28. [[CrossRef](#)] [[PubMed](#)]
162. Wang, Y.; Zhang, X.; Zhao, L.; Bao, T.; Wen, W.; Zhang, X.; Wang, S.-F. Integrated amplified aptasensor with in-situ precise preparation of copper nanoclusters for ultrasensitive electrochemical detection of microRNA 21. *Biosens. Bioelectron.* **2017**, *98*, 386–391. [[CrossRef](#)] [[PubMed](#)]
163. Smith, D.A.; Newbury, L.J.; Drago, G.; Bowen, T.; Redman, J.E. Electrochemical detection of urinary microRNAs via sulfonamide-bound antisense hybridisation. *Sens. Actuators B Chem.* **2017**, *253*, 335–341. [[CrossRef](#)] [[PubMed](#)]
164. Ebrahimi, A.; Nikokar, I.; Zokaei, M.; Bozorgzadeh, E. Design, development and evaluation of microRNA-199a-5p detecting electrochemical nanobiosensor with diagnostic application in Triple Negative Breast Cancer. *Talanta* **2018**, *189*, 592–598. [[CrossRef](#)] [[PubMed](#)]
165. Duan, F.; Guo, C.; Hu, M.; Song, Y.; Wang, M.; He, L.; Zhang, Z.; Pettinari, R.; Zhou, L. Construction of the 0D/2D heterojunction of Ti₃C₂T_x MXene nanosheets and iron phthalocyanine quantum dots for the impedimetric aptasensing of microRNA-155. *Sens. Actuators B Chem.* **2020**, *310*, 127844. [[CrossRef](#)]
166. Yaman, Y.T.; Vural, O.A.; Bolat, G.; Abaci, S. One-pot synthesized gold nanoparticle-peptide nanotube modified disposable sensor for impedimetric recognition of miRNA 410. *Sens. Actuators B Chem.* **2020**, *320*, 128343. [[CrossRef](#)]
167. Yammouri, G.; Mandli, J.; Mohammadi, H.; Amine, A. Development of an electrochemical label-free biosensor for microRNA-125a detection using pencil graphite electrode modified with different carbon nanomaterials. *J. Electroanal. Chem.* **2017**, *806*, 75–81. [[CrossRef](#)]
168. Voccia, D.; Sosnowska, M.; Bettazzi, F.; Roscigno, G.; Fratini, E.; De Franciscis, V.; Condorelli, G.; Chitta, R.; D'Souza, F.; Kutner, W.; et al. Direct determination of small RNAs using a biotinylated polythiophene impedimetric genosensor. *Biosens. Bioelectron.* **2017**, *87*, 1012–1019. [[CrossRef](#)]
169. Mandli, J.; Amine, A. Impedimetric genosensor for miRNA-34a detection in cell lysates using polypyrrole. *J. Solid State Electrochem.* **2017**, *22*, 1007–1014. [[CrossRef](#)]
170. Meng, T.; Zhao, D.; Ye, H.; Feng, Y.; Wang, H.; Zhanga, Y. Construction of an ultrasensitive electrochemical sensing platform for microRNA-21 based on interface impedance spectroscopy. *J. Colloid Interface Sci.* **2020**, *578*, 164–170. [[CrossRef](#)]
171. Zhang, J.; Wu, D.-Z.; Cai, S.-X.; Chen, M.; Xia, Y.-K.; Wu, F.; Chen, J. An immobilization-free electrochemical impedance biosensor based on duplex-specific nuclease assisted target recycling for amplified detection of microRNA. *Biosens. Bioelectron.* **2016**, *75*, 452–457. [[CrossRef](#)] [[PubMed](#)]
172. Salimi, A.; Kavosi, B.; Navaee, A. Amine-functionalized graphene as an effective electrochemical platform toward easily miRNA hybridization detection. *Meas. J. Int. Meas. Confed.* **2019**, *143*, 191–198. [[CrossRef](#)]

173. Hu, F.; Zhang, W.; Zhang, J.; Zhang, Q.; Sheng, T.; Gu, Y. An electrochemical biosensor for sensitive detection of microRNAs based on target-recycled non-enzymatic amplification. *Sens. Actuators B Chem.* **2018**, *271*, 15–23. [[CrossRef](#)]
174. Bharti, A.; Agnihotri, N.; Prabhakar, N. A voltammetric hybridization assay for microRNA-21 using carboxylated graphene oxide decorated with gold-platinum bimetallic nanoparticles. *Microchim. Acta* **2019**, *186*, 185. [[CrossRef](#)] [[PubMed](#)]
175. Salahandish, R.; Ghaffarinejad, A.; Omidinia, E.; Zargartalebi, H.; Majidzadeh-A, K.; Naghib, S.M.; Sanati-Nezhad, A. Label-free ultrasensitive detection of breast cancer miRNA-21 biomarker employing electrochemical nano-genosensor based on sandwiched AgNPs in PANI and N-doped graphene. *Biosens. Bioelectron.* **2018**, *120*, 129–136. [[CrossRef](#)] [[PubMed](#)]
176. Boriachek, K.; Umer, M.; Islam, N.; Gopalan, V.; Lam, A.K.-Y.; Nguyen, N.-T.; Shiddiky, M.J. An amplification-free electrochemical detection of exosomal miRNA-21 in serum samples. *Analyst* **2018**, *143*, 1662–1669. [[CrossRef](#)]
177. Wan, Z.; Umer, M.; Lobino, M.; Thiel, D.; Nguyen, N.-T.; Trinchì, A.; Shiddiky, M.J.; Gao, Y.; Li, Q. Laser induced self-N-doped porous graphene as an electrochemical biosensor for femtomolar miRNA detection. *Carbon* **2020**, *163*, 385–394. [[CrossRef](#)]
178. Koo, K.M.; Carrascosa, L.G.; Shiddiky, M.J.A.; Trau, M. Poly(A) Extensions of miRNAs for Amplification-Free Electrochemical Detection on Screen-Printed Gold Electrodes. *Anal. Chem.* **2016**, *88*, 2000–2005. [[CrossRef](#)]
179. Kannan, P.; Maiyalagan, T.; Lin, B.; Lei, W.; Jie, C.; Guo, L.; Jiang, Z.; Mao, S.; Subramanian, P. Nickel-phosphate pompon flowers nanostructured network enables the sensitive detection of microRNA. *Talanta* **2020**, *209*, 120511. [[CrossRef](#)]
180. Gai, P.; Gu, C.; Li, H.; Sun, X.; Li, F. Ultrasensitive Ratiometric Homogeneous Electrochemical MicroRNA Biosensing via Target-Triggered Ru(III) Release and Redox Recycling. *Anal. Chem.* **2017**, *89*, 12293–12298. [[CrossRef](#)]
181. La, M.; Zhang, Y.; Gao, Y.; Li, M.; Liu, L.; Chang, Y. Impedimetric Detection of Micro RNAs by the Signal Amplification of Streptavidin Induced In Situ Formation of Biotin Phenylalanine Nanoparticle Networks. *J. Electrochem. Soc.* **2020**, *167*. [[CrossRef](#)]
182. Azzouzi, S.; Mak, W.C.; Kor, K.; Turner, A.P.; Ben Ali, M.; Beni, V. An integrated dual functional recognition/amplification bio-label for the one-step impedimetric detection of Micro-RNA-21. *Biosens. Bioelectron.* **2017**, *92*, 154–161. [[CrossRef](#)] [[PubMed](#)]
183. Low, S.S.; Pan, Y.; Ji, D.; Li, Y.; Lu, Y.; He, Y.; Chen, Q.; Liu, Q. Smartphone-based portable electrochemical biosensing system for detection of circulating microRNA-21 in saliva as a proof-of-concept. *Sens. Actuators B Chem.* **2020**, *308*, 127718. [[CrossRef](#)]
184. Yin, H.; Wang, M.; Yang, Z.; Lu, L.; Yin, H.; Ai, S. Electrochemical biosensor for microRNA detection based on hybridization protection against nuclease S1 digestion. *J. Solid State Electrochem.* **2015**, *20*, 413–419. [[CrossRef](#)]
185. Jeong, B.; Kim, Y.J.; Jeong, J.-Y. Label-free electrochemical quantification of microRNA-375 in prostate cancer cells. *J. Electroanal. Chem.* **2019**, *846*, 113127. [[CrossRef](#)]
186. Li, J.; Wang, Y.; Deng, R.; Lin, L.; Liu, Y.; Li, J. Carbon nanotube enhanced label-free detection of microRNAs based on hairpin probe triggered solid-phase rolling-circle amplification. *Nanoscale* **2015**, *7*, 987–993. [[CrossRef](#)]
187. Akbarnia, A.; Zare, H.R.; Moshtaghioun, S.M.; Benvidi, A. Highly selective sensing and measurement of microRNA-541 based on its sequence-specific digestion by the restriction enzyme HinfI. *Colloids Surf. B Biointerfaces* **2019**, *182*, 110360. [[CrossRef](#)]
188. Azab, S.M.; Elhakim, H.K.; Fekry, A.M. The strategy of nanoparticles and the flavone chrysin to quantify miRNA-let 7a in zepto-molar level: Its application as tumor marker. *J. Mol. Struct.* **2019**, *1196*, 647–652. [[CrossRef](#)]
189. Kangkamano, T.; Numnuam, A.; Limbut, W.; Kanatharana, P.; Vilaivan, T.; Thavarungkul, P. Pyrrolidinyl PNA polypyrrole/silver nanofoam electrode as a novel label-free electrochemical miRNA-21 biosensor. *Biosens. Bioelectron.* **2018**, *102*, 217–225. [[CrossRef](#)]
190. Yang, L.; Wang, H.; Lü, H.; Hui, N. Phytic acid functionalized antifouling conducting polymer hydrogel for electrochemical detection of microRNA. *Anal. Chim. Acta* **2020**, *1124*, 104–112. [[CrossRef](#)]

191. Zhu, D.; Liu, W.; Zhao, D.; Hao, Q.; Lianhui, W.; Huang, J.; Shi, J.; Chao, J.; Su, S.; Wang, L. Label-Free Electrochemical Sensing Platform for MicroRNA-21 Detection Using Thionine and Gold Nanoparticles Co-Functionalized MoS₂ Nanosheet. *ACS Appl. Mater. Interfaces* **2017**, *9*, 35597–35603. [[CrossRef](#)] [[PubMed](#)]
192. Zouari, M.; Campuzano, S.; Pingarrón, J.M.; Raouafi, N. Determination of miRNAs in serum of cancer patients with a label- and enzyme-free voltammetric biosensor in a single 30-min step. *Microchim. Acta* **2020**, *187*, 1–11. [[CrossRef](#)] [[PubMed](#)]
193. Sabahi, A.; Salahandish, R.; Ghaffarinejad, A.; Omidinia, E. Electrochemical nano-genosensor for highly sensitive detection of miR-21 biomarker based on SWCNT-grafted dendritic Au nanostructure for early detection of prostate cancer. *Talanta* **2020**, *209*, 120595. [[CrossRef](#)] [[PubMed](#)]

Publisher's Note: MDPI stays neutral with regard to jurisdictional claims in published maps and institutional affiliations.



© 2020 by the authors. Licensee MDPI, Basel, Switzerland. This article is an open access article distributed under the terms and conditions of the Creative Commons Attribution (CC BY) license (<http://creativecommons.org/licenses/by/4.0/>).